NOTCH SENSITIVITY OF FIBER REINFORCED COMPOSITE

by

Mostafa Elyoussef

A Thesis presented to the Faculty of the
American University of Sharjah
College of Engineering
In Partial Fulfillment
of the Requirements
for the Degree of

Master of Science in
Mechanical Engineering

Sharjah, United Arab Emirates

April 2019

Approval Signatures

We, the undersigned, approve the Master's Thesis of Mostafa Elyoussef

Thesis Title: Notch Sensitivity of Fiber Reinforced Composite

Signature	**Date of Signature** (dd/mm/yyyy)
_____	_____
Dr. Maen Alkhader Associate Professor, Department of Mechanical Engineering Thesis Advisor	
_____	_____
Dr. Wael Abuzaid Assistant Professor, Department of Mechanical Engineering Thesis Co-Advisor	
_____	_____
Dr. Bassam Abu-Nabah Assistant Professor, Department of Mechanical Engineering Thesis Committee Member	
_____	_____
Dr. Rami Haweeleh Professor, Department of Civil Engineering Thesis Committee Member	
_____	_____
Dr. Mamoun Abdel-Hafez Head, Department of Mechanical Engineering	
_____	_____
Dr. Lotfi Romdhane Associate Dean for Graduate Affairs and Research College of Engineering	
_____	_____
Dr. Naif Darwish Acting Dean, College of Engineering	
_____	_____
Dr. Mohamed El-Tarhuni Vice Provost for Graduate Studies	

Acknowledgment

I would like to express my deepest gratitude to my supervisors Dr. Maen Alkhader and Dr. Wael Abuzaid for their guidance, encouragement, and support throughout my research stages. I am deeply beholden for their worthy discussion and suggestions. It was really an honor to work under their supervision.

I would also like to thank the committee members for their valuable comments and suggestions.

I am also thankful to the professors of Mechanical engineering department who taught me Master level courses. I am confident that my experience at AUS has equipped me with the knowledge and set of skills needed to pursue my doctoral studies.

I am also grateful to Abdulla Al Ghurair Foundation for Education for awarding me the Al Ghurair STEM Program scholarship to pursue my Master's degree.

Heartfelt thanks go to my family members for their endless support and encouragements. They have always been my inspiration for success.

Dedication

To my family…

Abstract

In most applications, structures made of composite materials involve features such as drilled assembly holes, which induce stress concentrations in their vicinities resulting in a reduction in the load carrying capacity of the structure. The nature of the damage resulting from such geometric features in orthotropic CFRP composites has been the subject of extensive research. Nevertheless, few works have investigated the behavior of notched CFRP composites exposed to elevated temperatures. Accordingly, the aim of this research is to investigate the effect of elevated temperatures on the notch sensitivity of CFRP composites. To achieve the goal of this study, both the *nominal* and *local* responses of woven CFRP samples were experimentally investigated, with the aid of Digital Image Correlation technique (DIC). Tensile tests were conducted on notched (*i.e.* with circular hole) and un-notched samples at 25°C, 50°C, 75°C, and 100°C. The experimental results obtained from the global stress-strain response of un-notched samples showed a decreasing trend in the mechanical properties with increasing temperatures. However, the global response of notched samples at 50°C surprisingly deviated from the expected trend and exhibited higher tensile strength than that at 25°C. Moreover, the notch sensitivity, assessed through un-notched to notched strength ratio, was found to decrease with increasing temperatures. Fractured surface examination showed two different damage mechanisms: Transverse cracks and axial splitting. It was noticed that transverse cracks was evident at the four temperature levels, while axial splitting was absent at room temperature. Measuring the local axial strains at the transverse crack initiation site showed a clear deviation from the linear response at the onset of transverse cracking. Moreover, investigating the local response at the axial splitting initiation site revealed a sudden change in the transverse and shear strain evolution. The blunting effect of axial splitting was found to become more significant at higher temperatures. Furthermore, residual shear strains were measured at the end of loading-unloading cycle for different temperature levels. It was found that residual strains are negligible at room temperatures and become more significant at higher loading temperatures.

Keywords: ***CFRP; Notch sensitivity; Temperature; Axial Splitting; Transverse Cracks; Digital Image Correlation***

Table of Contents

List of Figures

List of Tables

Chapter 1. Introduction

1.1. Overview

Recently, Carbon fiber reinforced polymer composites (CFRP) have been increasingly replacing conventional structural metallic materials due to their desirable properties of high stiffness, corrosion resistance, and superior strength to weight ratio. Motivated by the weight reduction advantage, which can be translated into significant energy saving, CFRPs have received a considerable attention in the aerospace industry. Prominent examples highlighting the increase in the demand of CFRP include AIRBUS A350, where the percentage by weight of embedded composite in structural members has increased from 50 to 60% [1]. It has been estimated that reducing the weight of an Airbus A320 by 1 Kg can reduce energy consumption by an amount equivalent to that produced by 2900 liter of fuel [2]. Another example of the use of composite in aerospace application is the Boeing 787 which achieved a weight reduction of 20% due to the extensive employment of composite materials in different components (*e.g.*, drive shafts, transmission housing, rotors controls, blades and hubs) [3]. This growing demand and importance of CFRP composites rendered them as one of the fastest growing engineering materials. A recent study has predicted an increase in the value of global composite market by 10.9 billion dollars from 2011 to 2017 [4].

In most aerospace applications, the employment of fiber reinforced polymer requires the use of joints in wings and tail assemblies [5]. These joints play an important role in transferring load among several parts in the structure of the aircraft. Such assembly generally requires the presence of drilled holes for insertion of bolts and connections. However, the presence of these discontinuities induces stress concentration in their vicinity and leads to a reduction in the load carrying capacity of the structure. Moreover, stress and strain gradients near notches can interact with heterogeneities in composite materials leading to the development of complex damage mechanisms. Thus, numerous studies and experimental works have been performed to characterize the behavior of notched CFRP composites.

Under normal operational conditions, components made of CFRP composite materials can be exposed during their service life to different environmental elements

(*e.g.*, moisture absorption, UV radiation, and high temperatures). Significant efforts have been dedicated to investigate the effect of such environmental elements on the structural and mechanical properties of CFRP composites. However, few works have investigated the effect of these elements on the behavior of notched composite laminates. In particular, there is limited work focused on assessing the notch sensitivity and the development of damage in the vicinity of geometric discontinuities of CFRP at elevated temperatures.

1.2. Research Objectives

The main goal of the proposed work is to investigate the effect of elevated temperatures on the mechanical properties and notch sensitivity of woven CFRP composites. To satisfy this goal, the following sub-objectives need to be achieved:

- Develop a deep insight into the local response of the notched composite laminate using full-field measurement technique.
- Explore the effect of elevated temperature on the initiation and progression of different damage mechanisms.
- Compare the *nominal* and *local* behavior of woven CFRP composites at different temperature levels.
- Calculate stress concentration factor from the experimentally measured stain components.
- Study the consequence of damage progression on the local strain field in the adjacent regions of the damage.
- Assess the change in hole geometry due to the initiation and progression of damage

1.3. Research Contribution

The contribution of this thesis can be summarized as follows:

- Estimate notch sensitivity at different temperature levels by comparing notched and un-notched strengths of CFRP samples
- Utilize full-field measurement technique to provide qualitative and quantitative information about the damage mechanisms at different temperature levels.

- Assess the effect of elevated temperatures on the type and the extent of damage developed near the hole perimeter.
- Relate the evolution of different strain components to the initiation and progression of different damage mechanisms.
- Visualize the stress and strain relaxation resulting from damage initiation and progression
- Demonstrate blunting effect resulting from the progression of axial splitting damage mode, a type of damage in CFRP, at different temperature levels.

1.4. Thesis Organization

The rest of the thesis can be summarized as follows: Chapter 2 presents a literature review of some of the existing works studying the behavior of notched composite laminates and the associated damage mechanisms. It also provides a background about the effect of environmental elements, and particularly elevated temperatures, on the structural behavior of CFRP composites. Chapter 3 illustrates the experimental approach followed to satisfy the goal of this research. Chapter 4 describes the experimental set-up and procedures used to conduct the experimental work. Chapter 5 presents and discusses the experimental results. Chapter 6 summarizes the major findings of this research and proposes potential future works.

Chapter 2. Background and Literature Review

Investigating the behavior of composite laminate with discontinuities has been the concern of many researchers in the last decades. It has been found that the stress and strain gradients developed near the edge of a circular hole can interact with heterogeneities in the composite in a cooperative and complex manner leading to the initiation and progression of different damage mechanisms. For examples, notches are observed to cause matrix cracking in the off-axis plies, while in 0° plies cause axial splitting and delamination. The initiation and the progression of the damage mechanisms can cause stress and strain relaxation near the notch resulting in a higher notched strength. The degree of the stress redistribution is mostly controlled by the type and the extent of damage developed in the vicinity of the hole. However, the initiation and progression of damage mechanisms can also be significantly affected by a number of factors, such as: lay-up configuration, notch geometry, loading rate, specimen thickness, and constituent material [6].

2.1. Effect of Different Factors on the Damage Mechanisms and the Notch Sensitivity of Notched Composite Laminates

The effect of laminate lay-up and stacking sequence has been thoroughly investigated by a number of researchers [7-10]. An experimental study performed by Harris and Morris [8] revealed that both fiber orientation and stacking sequence can significantly affect the notch sensitivity and the extent of damage in CFRP composites. It has been also shown that axial splitting damage mode exhibited by the 0° ply can effectively alleviate the overstress developed near the hole edge. Another study conducted by Kortschot & Beaumont [9] demonstrated that composite laminate with ($[90°_2/0°_2]_s$) lay-up configuration exhibited higher extent of damage and thus higher notch sensitivity than the ($[90°/0°]_{2s}$) laminate, indicating that the order of plies (*i.e.* stacking sequence) can have significant effect on the behavior of notched composite laminate.

Laminate thickness has been also found to affect the notch sensitivity of composite materials. By increasing the laminate thickness, the extent of damage is reduced and confined to the outer plies only [11]. However, according to the type of damage experienced by the different lay-up configurations, the notched strength was found to increase or decrease as the number of plies increases (*i.e.* thickness

increases). Nevertheless, beyond a certain number of plies, the notched strength becomes independent of the laminate thickness.

Numerous studies have been performed to evaluate the effect of hole size on the notched strength of composite laminates [12-14]. It was shown that the notched strength decreases as the hole size increases. This was rationalized based on the fact that the maximum strain/stress at the hole tip decreases more steeply as the hole size decreases, indicating that the high axial strain region is larger in a specimen with greater hole size. The larger strain region can cause larger crack to form near the hole, leading to a reduction in the notched tensile strength. This indicates that the damage is not always beneficial in decreasing the notch sensitivity through blunting.

The effect of constituent material on the notch sensitivity of composite laminates was also investigated. A study was conducted by Pinnel [15] to evaluate the behavior of notched composite laminate in two material systems: thermoplastic and thermoset. The experimental results showed that the thermoplastic laminate exhibits higher open-and filled-tensile strength than the thermoset laminate. This observation was attributed to the higher ductility of thermoplastic matrix compared to thermoset matrix, which results in a higher stress relief near the hole edge.

Significant efforts have been exerted to characterize the effect of different variables on notch sensitivity and the development of damage mechanisms associated with notches in CFRP composites. As notch sensitivity is greatly influenced by the type and the extent of damage accumulated in the vicinity of the notch, it is crucial to track the initiation and the progression of different damage mechanisms. Thus, various experimental techniques have been employed to monitor the development of damage during loading. For example,

Perry [16], used moire interferometry to examine the damage progression in notched ceramic matrix material. He found that the strain levels near the notch remain low even with increasing load, which can be explained by the stress redistribution that is taking place due to the extensive matrix cracking that acts as strain relief for the composite.

Hallet et al. [17] carried out a study to investigate the progressive damage development in composite laminates with circular holes through the use of non-

destructive techniques (X-rays and CT scanning). By performing an interrupted testing on open hole tensile specimen, he was able to determine the damage progression sequence within the specimen as load was increased. First, he found that damage initiates at the hole edge in the form of matrix cracking in the off-axis plies. As load increases, more extensive damage takes place in the form of delamination which in turn propagates through the thickness of specimen and causes stress relief by axial splitting. In the final stage, damage takes place throughout the whole section far from the stress concentrators. These experimental observations showed a close match with the results obtained by FE models that account for delamination and axial splitting using interface elements and model fiber failure using the Weibull distribution.

Caminero et al. [18] conducted an experimental study to examine the damage mechanisms taking place during the tensile loading of a notched composite laminate having different stacking sequences using digital image correlation technique. X-radiography was also employed to help in identifying damage positions and in correlating them with the high strain regions detected by digital image correlations (DIC). The high localized strain captured by DIC showed good agreement with the damage positions obtained from X-radiography. The strain maps show high localized strain near the hole and in a direction parallel to the fiber orientation. The results obtained by the two techniques indicate that the dominant damage mechanism depends mainly on the ply stacking sequence. Axial splitting, resulting from high shear and transverse strains, was the main damage type observed in unidirectional laminates with $[0°]_8$ ply sequence. On the other hand, matrix cracking driven by high axial strain was the main damage mode taking place in laminates with $[90°]_8$ ply sequence. The DIC strain maps of laminates with $[0°/90°]_{2s}$ ply sequence show high values of axial and shear strains which led to a combination of axial splitting and transverse cracking damage modes as shown by the X-radiographs. It was also concluded that the notch sensitivity is directly affected by the damage mechanisms taking place during loading.

Another study that employed the full-field strain measurement technique was performed by Pierron et al. [19] to investigate the damage development in a glass-epoxy quasi-isotropic laminate under uniaxial tensile loading. It was shown that

cracks can be easily detected using the grid method and that cracks opening can be measured as a function of the applied stress. It was also noticed that crack opening is not always monotonic (strictly increasing) which can be related to the interaction between the initiation and the propagation of other cracks. Non-linear behavior of the material was also detected at the hole in the transverse direction. This non-linearity, represented by the high strain level in the strain maps, can be related to the crack formation in the 90° plies as revealed by microscopic observation. Strain redistribution was also obvious in the strain map.

The aforementioned studies provided valuable findings regarding damage initiation and progression near notches in composite laminates. They also showed that full-field measurement techniques are instrumental for identifying and monitoring the progression of damage mechanisms near notches, which can progress in a very complex manner. However, damage progression complexity can even be further complicated, and probably accelerated, by interacting with damages ensuing from exposure to environmental elements. A review of the efforts exerted to address the synergistic interaction between environmental elements and notches is provided next.

2.2. Environmental Elements

In aerospace applications, various components fabricated from composite materials are susceptible to harsh environmental elements such as: UV radiation, moisture absorption, and elevated temperatures. Siginifcant efforts have been exerted to characterize the effects of these environmental elements on the structural behavior of CFRP composites. It has been shown that the exposure to the aformentioned environmental elements can lead to siginificant degradation in the load-bearing abilities of CFRP composites [20-23]. More specifically, Exposure to UV radiation and moisture absorption was found to induce localized effect in CFRP composites. For example, mositure absorption can cause plasticisation, micro-cracks, and hydrolysis [20,21] while exposure to UV radiation can promote the formation of the surface micro-cracks [22]. However, it is worth mentioning that the induced damage mechanisms were observed to be confined to the exposed region, while the bulk of the material was not affected [24]. Accordingly, long-term damage accumalation is needed for noticeable degradation in the mechanical properties, as observed in different experimental studies [20-22]. Additionally, protective coatings are most

often employed to block moisture diffusion and UV radiation and thus protect the exposed surface from induced localized damages; therby improving the long-term durability and structural integrity of CFRP composites. On the other hand, sudden changes in temperatures can significantly and rapidly alter the structural properties of CFRP composite resulting in a catastrophic and unpredictble failure. Therefore, it is insturmental to have a better understanding of CFRP composites's behavior under elevated temperature levels.

The effect of elevated temperatures on the structural behavior and the mechanical properties of CFRP composites has been long observed. It has been found that exposure to high temperatures can adversly degrade the load-bearing capacity (*i.e.* Strength, Stiffness, Structural properties) of CFRP composites. For examples, numerous studies have demonstrated the reduction in tensile, compressive and shear strength at elevated temperatures [25-27]. The loss in the aformentioned mechanical properties becomes substational beyond the glass transition temperature (Tg), at which the ploymer is transformed from the glassy elastic to the rubbery state. Furthermore, the flexural behavior under elevated temperatures has been explored in a recent study performed by Abdalrahman [28]. The experimental results revealed a decreasing trend in the flexural stiffness and strength with the increase in temperatures from room temperatures to 90°C. Moreover, A substational reduction in the flexural properties was observed upon temperature rise from 75°C to 90°C, which was attributed to the thermal softening of the epoxy matrix that becomes more pronounced as the deformation temperature gets closer to the heat deflection temperature (HDT).

The significant degradation in the mechanical properties can be directly linked to the internal stresses induced in the polymer matrix and at the fiber/matrix interface due to the different thermal coeffcients of polymer matrix and reinforecement [29-30] . The magnitude of this internal stresses is highly dependent on the temperature level and can cause chemical bond disintegration at the fiber-matrix interface upon exposure to elevated temperatures.

The fracture properties of CFRP composites have also been investigated through experimental study conducted by Marom [31]. It has been shown that that the

interlaminate fracture energy can be reduced by up to 30% as a result of temperature rise from -50°C to 100°C. Moreover, the assessment of fracture surface characteristics revealed noticeable changes in the extent of fiber/matrix separation and resin fracture with the increase in temperature.

Although significant efforts have been made to characterize the performance of CFRP composites under elevated temperatures, the notched behavior of CFRP composites is still not well investigated at elevated temperature. The progress of the different damage mechanisms in the vicinity of the hole can be further complicated and probably accelerated by interacting with damage mechanisms induced by exposure to high temperatures. Thus, it is instrumental to address the synergistic interaction between temperature and notches on the structural properties of CFRP composites. Accordingly this work aims to address the consequence of this potential synergy on the local and global response of CFRP composites.

Chapter 3. Methodology

3.1. Experimental Approach

The adopted approach is purely experimental and designed to investigate the synergistic effect of temperature and notches on the structural behavior of Carbon fiber reinforced polymers (CFRP) composites. It is based on testing notched (*i.e.,* drilled circular hole) and un-notched samples under tensile uniaxial loading and in a temperature-controlled environment. Subsequently, the global and local responses are monitored at different temperatures to ascertain the temperature effect on the notch sensitivity of the studied composite laminate. As the material behavior is rather complex in the vicinity of the hole due to the development of stress gradient and the interaction of different damage mechanisms, it is instrumental to monitor the localized behavior in this region. Thus, a full-field measurement technique is employed in this study to provide local measurements and gain better insight into the development of damage mechanisms at different temperatures.

3.2. Digital Image Correlation Technique

An effective technique that allows for monitoring the material behavior and collecting full-field measurements at different length scales is digital image correlation (DIC). The principle of DIC is based on comparing the gray scale values of two monochromatic optical images of the sample's surface captured pre and post deformation as demonstrated in Figure 3.1. This comparison is enabled by the presence of distinctive features (*i.e.,* speckle pattern) on the surface of the studied material. However, if these features don't naturally exist on the surface, a random pattern should be applied to the area of interest. These unique features are tracked using correlation algorithm to determine the displacement fields at a given state. Subsequently, the computed displacement fields can be utilized for post-processing analysis and to generate full-field strain measurements through differentiation [32]. The tracking process is performed by taking small subsets of the reference images and then finding their corresponding location in the current image. Figure 3.2 illustrates the idea of tracking subsets. It is noteworthy to mention that the level of details that can be resolved using DIC is highly dependent on the pattern size and distribution as well as the level of magnification at which images are captured. Thus, it is important to optimize the pattern quality (speckles size and distribution) and choose the

appropriate magnification level. The use of DIC technique is instrumental in this study as it can provide better understanding of the local material response, particularly in the vicinity of the hole, through measuring all deformation fields in the entire region of interest. Such full-field DIC measurements are advantageous and preferable over strain gauges which can only provide point measurement at their location and in a single direction.

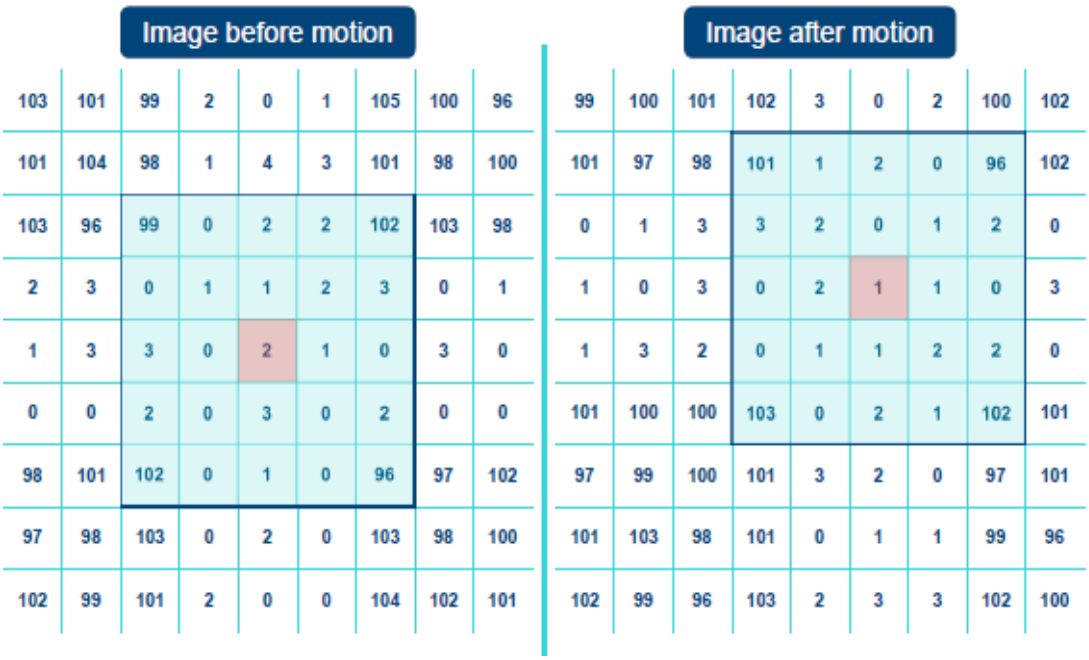

Figure 3.1: Comparing gray scale values of two monochromatic optical images captured before and after deformation [32]

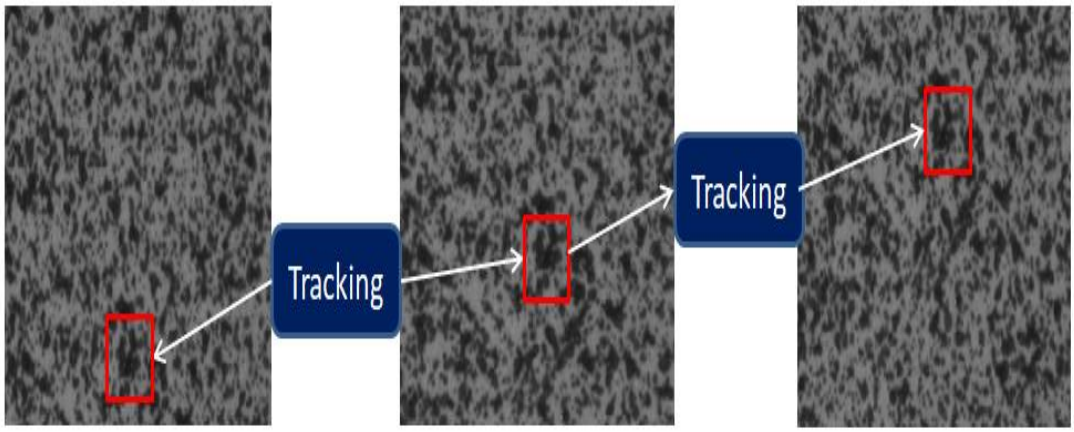

Figure 3.2: Tracking the location of small subset in the deformed image

3.3. Material Selection and Sample Preparation

For experimental practicality (*i.e.*, sample availability, repeatability of the results and avoiding complexities associated with the hand lay-up process of thin fabric ply), high quality woven CFRP composite sheet was acquired from Easy Composites, UK. This material was selected due to its wide use and its balanced properties, high quality, consistency and reliability. The considered composite laminate consists of 3 carbon fabric layers (2/2 twill, ±45, 2/2 twill) and epoxy resin matrix with a quasi-isotropic lay-up and 1 mm nominal thickness. Two sets of samples were used in this study: Notched (with circular hole) and Un-notched samples. As the aim of this study is to investigate the sole effect of temperature on the notch sensitivity, only one hole diameter to width ratio was considered; thus eliminating the hole size factor from this study. All samples (notched and un-notched) have a length of 160 mm and width of 20 mm. The samples were cut into the desired dimensions using shear cutting machine within an accuracy of $\pm 2\%$. To adequately understand the role of temperature in altering the notch sensitivity, the size of the hole was selected such that it results in a relatively high notch sensitivity factor, based on a previous study documented in the literature [33]. Thus, 3 mm circular hole was drilled at the center of the specimen resulting in hole diameter to width ratio of 0.15. To minimize damage initiation in the vicinity of the hole during drilling process, the sample was sandwiched between 2 wood pieces and drilled using CNC machine. Schematic drawings of un-notched and notched specimen are presented in Figures 3.3 and 3.4 respectively. Four tabs of 30 mm length were attached to both ends of the specimen using thin even layer of a temperature-resistant glue to ensure load distribution and prevent sample damage due to gripping. Binder clamps were also used to provide pressure on the end tabs and ensure adequate contact with the specimen surface. To prepare the samples for DIC correlation, they were first coated with while paint and then randomly sprayed with black aerosols using high quality air brush to effectively control the speckle size and distribution. An image of the painted surface is shown in Figure 3.5. To satisfy the goal of this research and thoroughly understand the effect of temperature on the notch sensitivity of CFRP composite, 4 different temperature levels (25 °C (room temperature), 50°C, 75°C, 100°C) were considered. Three samples (notched and un-notched) were used for each test scenario to ensure accuracy and repeatability of the results.

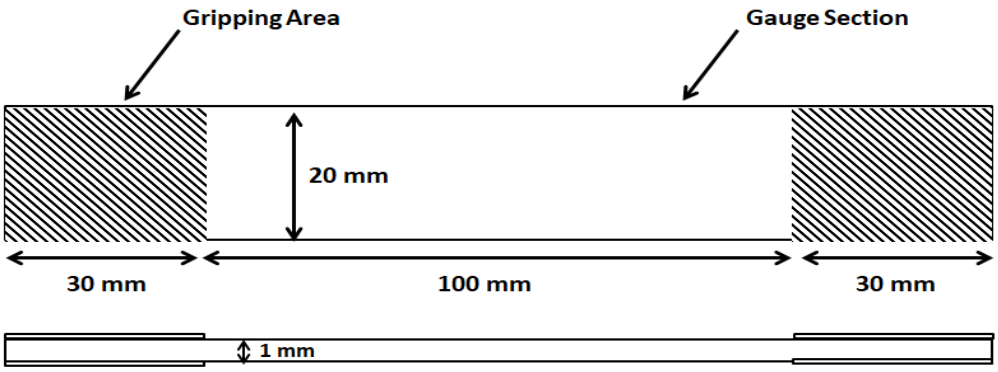

Figure 3.3: Un-notched sample configuration

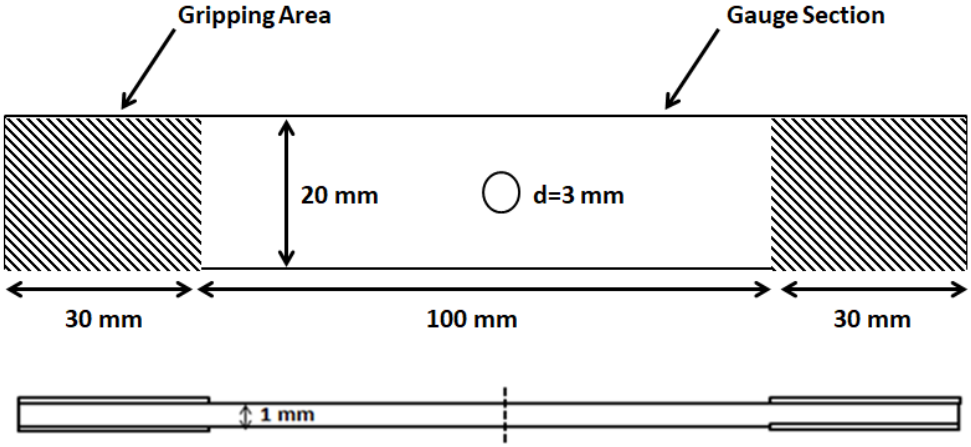

Figure 3.4: Notched sample configuration

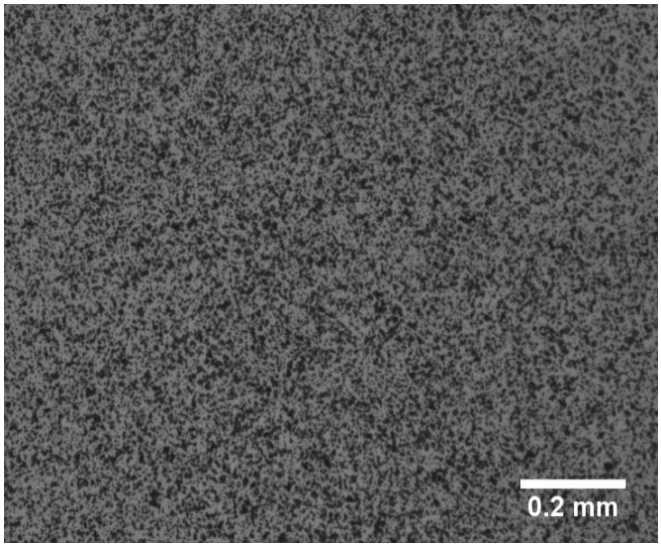

Figure 3.5: Surface pattern of un-notched specimen

Chapter 4. Experimental Set-up and Procedure

4.1. Experimental Setup and Tensile Testing

The experimental setup is comprised of the DIC system (Camera, Lens, Translation stage, Tripod, and Light source), 100 kN capacity Instron UTM, and an environmental chamber as shown in Figure 4.1. The specimen was properly aligned and tightly fixed using wedge grips. Prior to testing, sample was pre-conditioned in the environmental chamber for 30 minutes to ensure that the sample temperature has reached to the desired set point. Uniform illumination of the specimen was provided using LED light source. The position and the orientation of the camera were then calibrated using translation stages. The camera focus and light intensity were also adjusted before starting the test. All tests were displacement-controlled and conducted at crosshead rate of 1mm/min. During deformation, images were captured at a rate of 1 image/sec. The captured images were subsequently correlated using Vic-2D from correlated solution.

Figure 4.1: Experimental setup

4.2. Dynamic Mechanical Test

Glass transition temperature is the temperature range over which the material transitions from solid into rubbery state. To determine the glass transition temperature (Tg) of the considered composite laminate, Dynamic mechanical test (DMA) was performed. DMA is a dynamic measurenment technique where small osciallatory stress is applied to a sample with known geometry. The resulting strain can then be measured to determine the visco-elastic properties of the materials. These properties comprise the following:

1. **Storage modulus (E'')**: Elastic component related the material's stiffness.
2. **Loss modulus (E')**: Visocous component used to evaluate the material's ability to dissipated energy.
3. **Tangent (delta)**: Tangent of the Phase difference between strain and stress wave which describes the relation between elastic and in-elastic components.

Figure 4.2 shows the variation of the aformentioned properties as a function of the temperature. It can be noticed from the storage modulus curve that glass transition occurs between 62.652° Cand 100° C. However, a single value is usually used to indicate the glass transition point.Thus, the temperature at the loss modulus peak (70° C) is assumed to be the glass transiton temperature of the studied composite laminate.

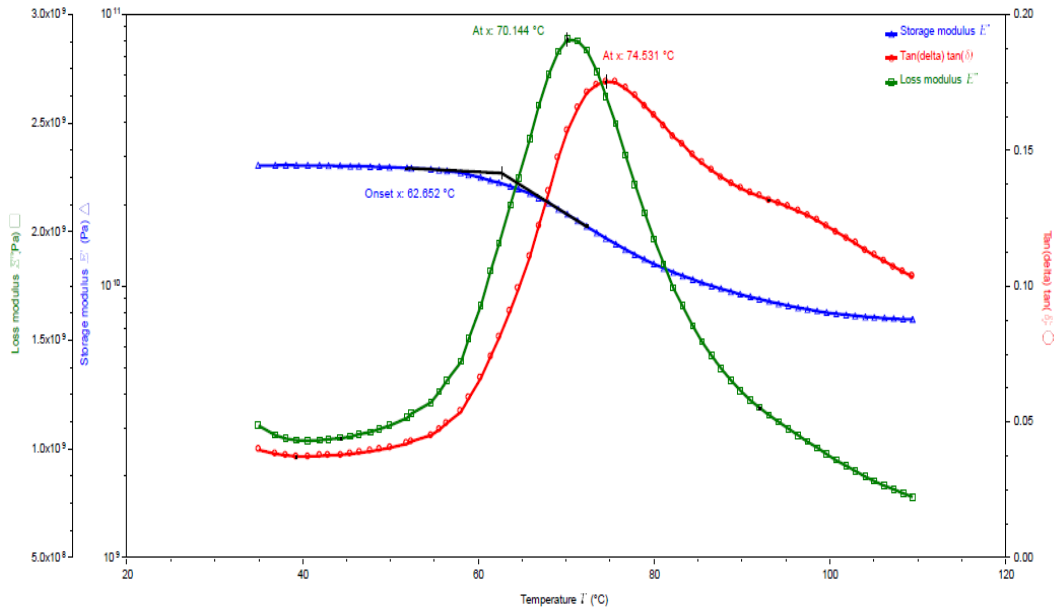

Figure 4.2: Variation of storage modulus, loss modulus, and tangent of phase angle as a function of temperature

Chapter 5. Results and Discussion

5.1. Determination of Elastic Constants

The mechanical properties of the studied composite laminate were determined by conducting tensile tests at 4 different temperature levels. Uniaxial tensile tests were performed to determine the modulus of elasticity and the ultimate tensile strength. Average strains were acquired from DIC correlation, and the corresponding stresses were computed by dividing the force recorded by the load cell of the UTM over the nominal cross-sectional area of the specimen. To find the longitudinal modulus of elasticity, tensile tests along the fiber direction were performed. Subsequently, axial stresses (*i.e.* along fiber direction) were plotted as a function of the average vertical strains acquired from DIC correlation. The modulus of elasticity was then determined by calculating the slope of the stress-strain curves, as shown in Figure 5.1. The transverse modulus of elasticity was assumed to be equal to the longitudinal modulus of elasticity due to the symmetry of the laminate. Poisson ratio was determined by plotting the transverse strains as a function of the longitudinal strains and then computing the initial slope of the curve, as illustrated in Figure 5.2.

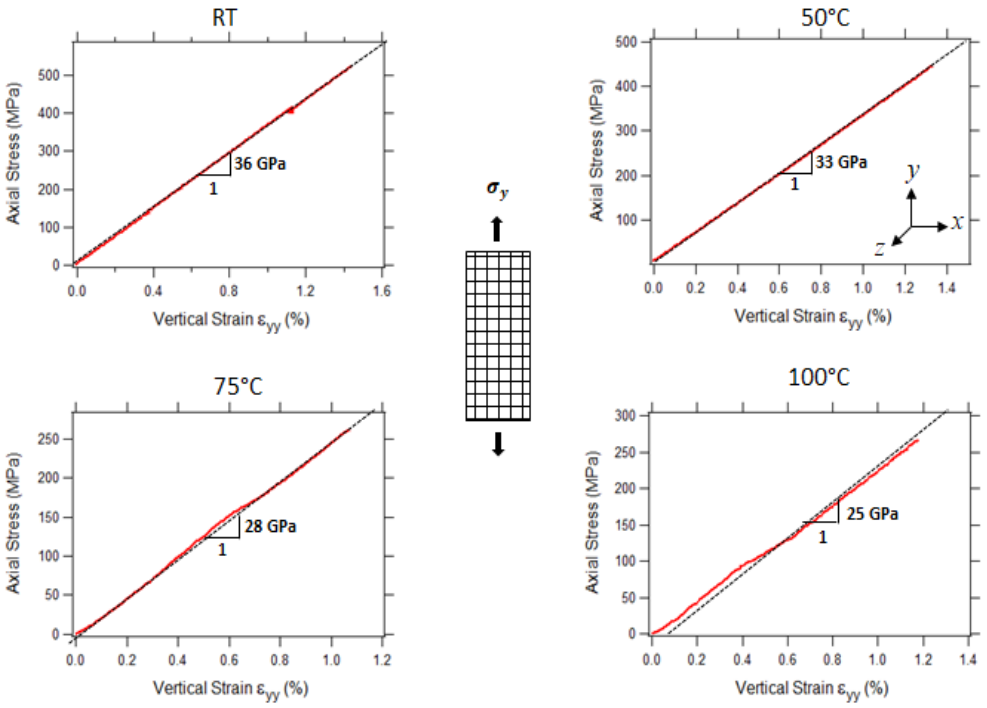

Figure 5.1: Determination of longitudinal modulus of elasticity

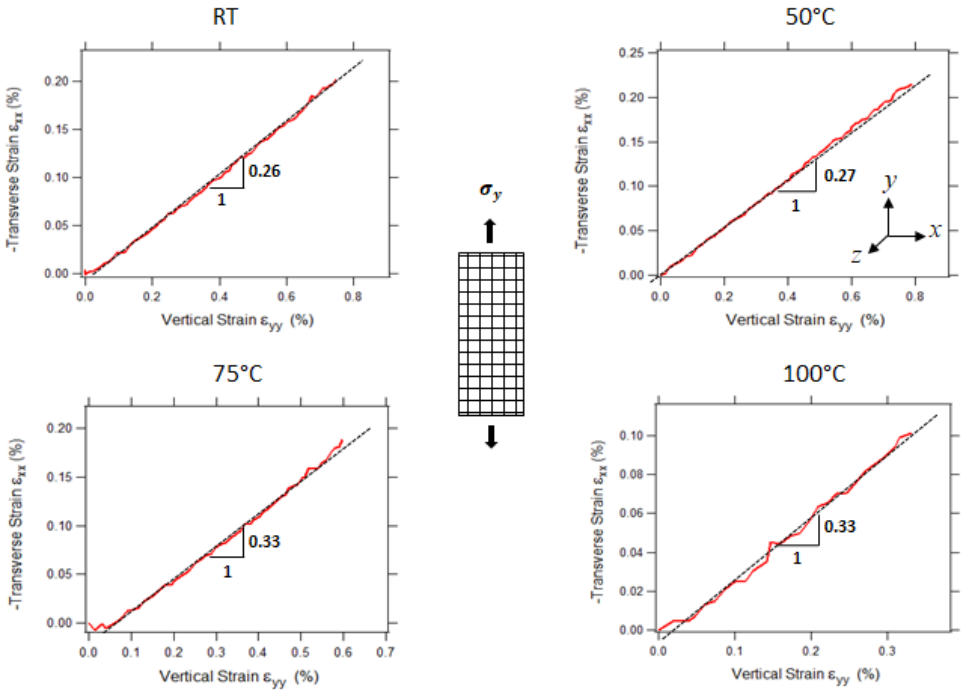

Figure 5.2: Determination of Poisson's ratio

To determine the shear modulus of elasticity, Hook's law given by equation (1) can be applied. To use Hook's law for shear stresses, off-axis loading (*i.e.* loading axis is not parallel to fiber direction, as illustrated in Figure 5.3) should be applied to the sample. Subsequently, stress and strain transformation given by equations (2) and (3) can be used to calculate shear stresses and shear strains along the fiber directions. Figure 5.4 shows the stress components before and after transformations.

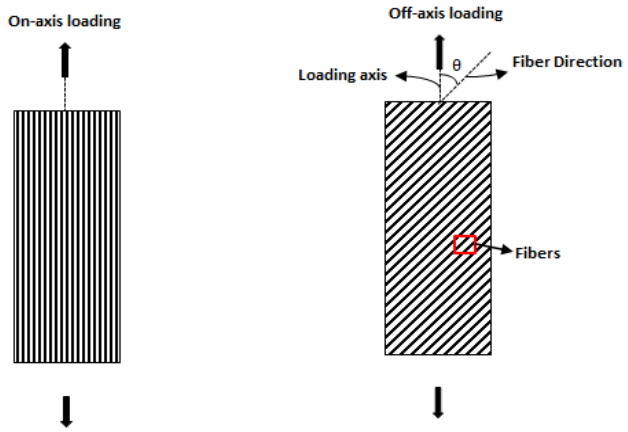

Figure 5.3: Schematic drawing showing the difference between on-axis and off-axis loading

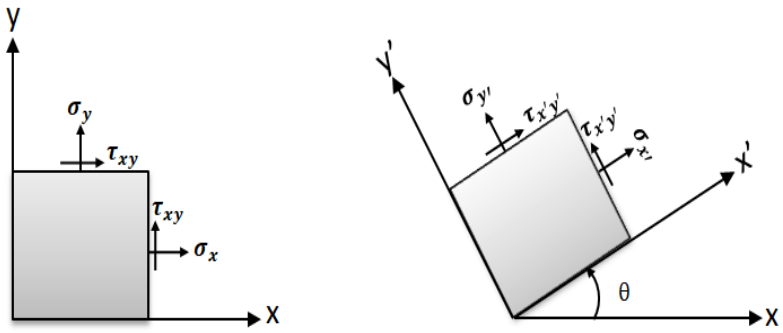

Figure 5.4: Stress components before and after transformation

Hook's Law: Applied stresses are proportional to the resulting strains within the elastic limit of the material used.

$$\tau = G\gamma \tag{1}$$

where τ is the shear stress, γ is the shear strain, and G is the shear modulus of elasticity

Stress Transformation: It is used to compute stress components in the x'y' plane oriented at an angle θ with respect to the x-axis.

$$\begin{Bmatrix} \sigma_{x'} \\ \sigma_{y'} \\ \tau_{x'y'} \end{Bmatrix} = \begin{bmatrix} c^2 & s^2 & 2sc \\ s^2 & c^2 & -2sc \\ -sc & sc & c^2 - s^2 \end{bmatrix} \begin{Bmatrix} \sigma_x \\ \sigma_y \\ \tau_{xy} \end{Bmatrix} \tag{2}$$

where $c = \cos\theta$ and $s = \sin\theta$

Strain Transformation: It is used to compute strain components in the x'y' plane oriented at an angle θ with respect to the x-axis.

$$\begin{Bmatrix} \varepsilon_{x'} \\ \varepsilon_{y'} \\ \frac{\gamma_{x'y'}}{2} \end{Bmatrix} = \begin{bmatrix} c^2 & s^2 & 2sc \\ s^2 & c^2 & -2sc \\ -sc & sc & c^2 - s^2 \end{bmatrix} \begin{Bmatrix} \varepsilon_x \\ \varepsilon_y \\ \frac{\gamma_{xy}}{2} \end{Bmatrix} \tag{3}$$

To determine the shear modulus of elasticity of the considered composite laminate, 45° off-axis tensile tests were conducted. Stress-Strain transformations given by equations (2) and (3) were then applied, after substituting $\theta = 45°$, to determine the shear stresses and shear strains in the plane oriented 45° from the loading axis (*i.e.* along the fiber direction) . Shear stresses were then plotted against shear strains, and the initial slope of the stress-strain curve was then computed to find

the in-plane shear modulus of elasticity, as shown in Figure 5.5. The determined elastic constants at the four temperature levels are summarized in Table 5.1.

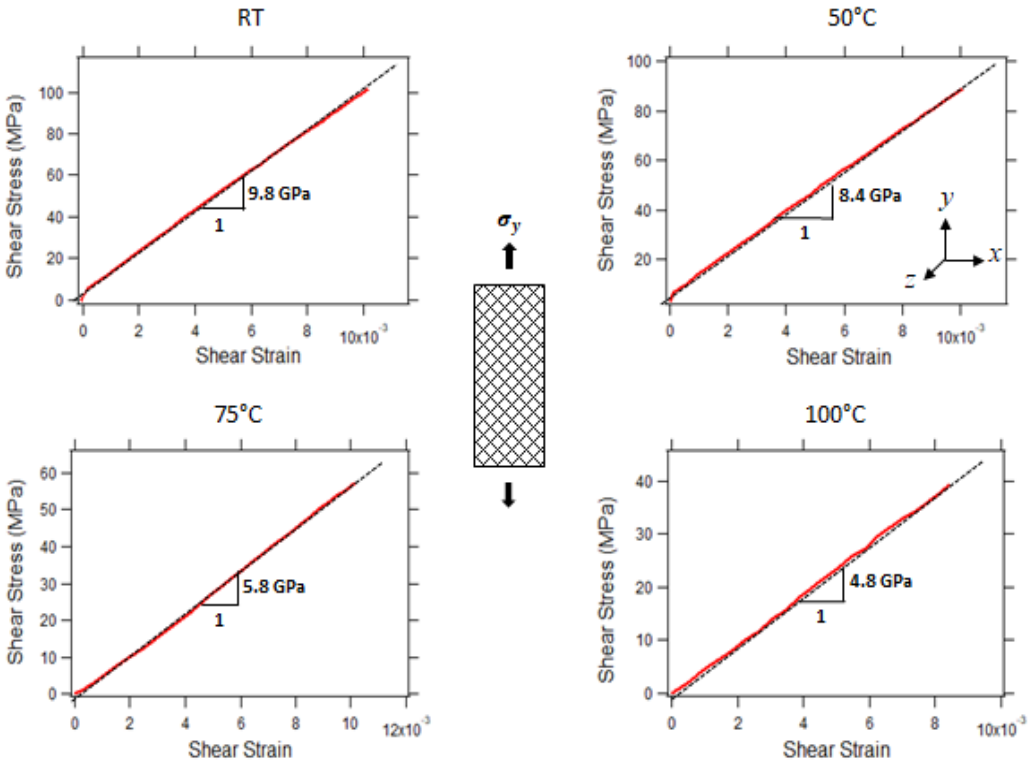

Figure 5.5: Determination of shear modulus of elasticity

Table 5.1: Mechanical properties at different temperature levels

Temperature	RT	50°C	75°C	100°C
longitudinal Modulus (GPa)	36	33	27	25
Transverse Modulus (GPa)	36	33	27	25
Shear Modulus (GPa)	9.8	8.4	5.8	4.8
Poisson Ratio	0.26	0.27	0.33	0.33

5.2. Effect of Temperature on the Global Response

To ascertain the effect of temperature on the global response of CFRP composites, nominal stresses were plotted against average strains for un-notched and notched samples, as shown in Figures 5.6 and 5.7 respectively. Average strain over the region of interest was acquired from DIC correlations, and corresponding stresses were computed by dividing the load measured by the load cell over the nominal cross-

sectional area (i.*e.*, Un-notched Area) of the sample. The stress-strain behavior of the un-notched samples, presented in Figure 5.6, shows a decreasing trend in both the ultimate tensile strength and the modulus of elasticity with increasing temperature. A reduction of about 8% in modulus of elasticity and 11% in ultimate tensile strength with respect to those of the virgin sample was observed upon increasing the test temperature to 50 °C. Further increase in the temperature beyond the glass transition point (T_g=70° C) resulted in a significant reduction in the aforementioned mechanical properties. This is demonstrated by a reduction of about 25% in the modulus of elasticity and 44% in the ultimate tensile strength at 75°C. However, increasing the test temperature further to 100 °C, showed a relatively small drop (*i.e.*, with respect to 75°C) in the mechanical properties, which is manifested by a drop of 31% in the modulus of elasticity and 47.1% in the tensile strength. The observed loss in the mechanical properties can be attributed to the thermal softening in the epoxy matrix that takes place at elevated temperatures. It is worth mentioning that this softening process becomes more significant beyond the glass transition temperature resulting in a substantial degradation in the mechanical properties. Moreover, unlike the linear elastic behavior observed at room temperatures and 50°C, the material behavior at 75°C and 100°C was found to exhibit non-linearity beyond a certain stress level. This non-linearity can be attributed to the significant matrix softening that takes place beyond the glass transition point. Similarly, the modulus of elasticity of notched samples was shown to decrease with increasing temperature. Furthermore, the ultimate notched tensile strength was observed to decrease significantly at 75°C and 100°C. However, the global response at 50°C was quite different and surprisingly deviated from the expected trends. The notched material exhibited higher tensile strength at 50°C than at room temperature. This increase in the ultimate tensile strength at 50°C is unpredictable since the thermal softening is expected to cause a reduction in both the ultimate tensile strength and the modulus of elasticity. Hence, the obtained results highlight the presence of another factor counteracting the consequence of softening. A possible explanation for this behavior is the reduction in the stress concentration associated with the presence of the geometric feature (*i.e.*, drilled hole) due to the increase in temperatures, which will consequently delay the onset of the final failure. This increase in the tensile strength is expected to overcome the reduction in the tensile strength caused by thermal softening at 50°C. It is

emphasized here that the observations made in Figures 5.6 and 5.7 were made based on at least 3 specimens for each sample geometry and deformation temperature.

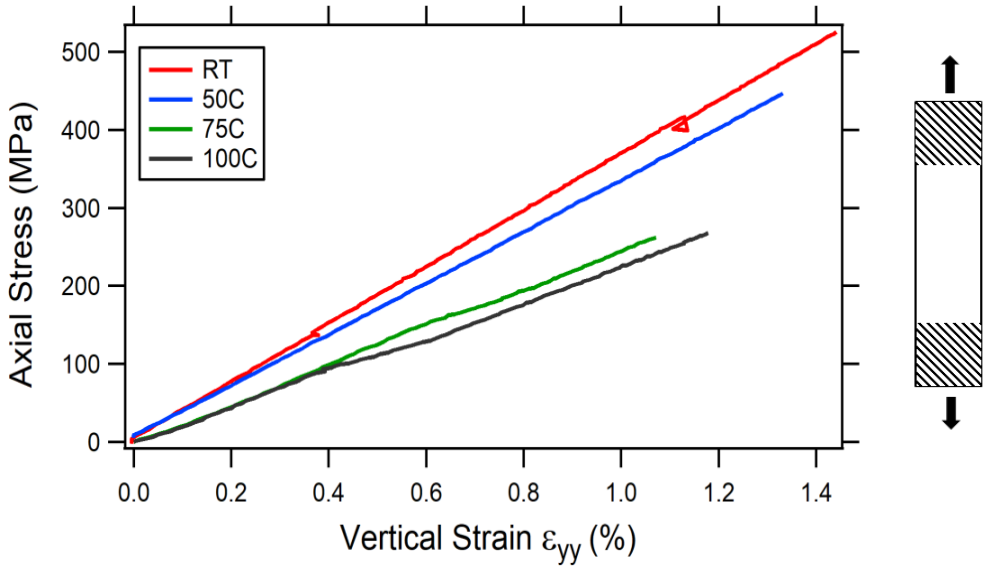

Figure 5.6: Stress-strain curves of un-notched specimen at different temperatures

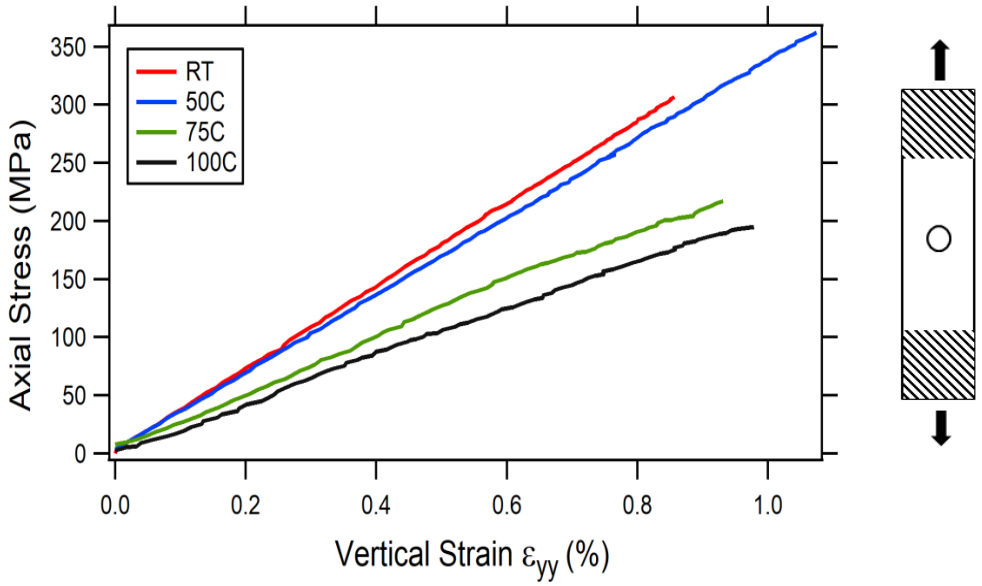

Figure 5.7: Stress-strain curves of notched specimen at different temperatures

To assess change in the notch sensitivity with temperature variation, the ratio of un-notched tensile strength (Su) to the notched tensile strength (Sn) was computed at the four temperature levels. The results are summarized in Table 5.2. It can be clearly inferred from the tabulated values that the notch sensitivity (Su/Sn) decreases with the increase in temperature. It is also worth mentioning that Su/Sn becomes very

close to 1 at 75°C and 100°C indicating that the notch becomes almost insensitive at temperatures beyond the glass transition point.

Table 5.2: Investigating the notch sensitivity at the different temperature levels

Temperature	RT	50° C	75° C	100° C
Un-notched Strength Su (MPa)	512	456	271	268
Notched Strength Sn (MPa)	368	414	262	265
Su/Sn	1.39	1.105	1.034	1.01

Notch sensitivity is primarily dependent on the extent of stress relaxation that takes place in the vicinity of the hole. It is well known that stress relaxation is a consequence of damage initiation and progression. Thus, it is instrumental to investigate the extent and the type of damage mechanisms at different temperatures and assess their effect on the notch sensitivity. This aspect will be addressed in Section 5.3 of this thesis.

5.3. Final Failure of the Sample at Different Temperature Levels

Figures 5.8-5.11 display the final fractured surfaces of representative samples deformed at the four temperature levels. Inspecting the surface of the damaged sample reveals the presence of axial (*i.e.* parallel to the loading direction) splitting and transverse cracks (*i.e.*, perpendicular to the loading direction) in the vicinity of the drilled holes. Moreover, it can be clearly noticed that at room temperature, axial splitting is not evident on the surface of the sample. However, this damage mode becomes noticeable at higher temperatures. It is also worth mentioning that at 100°C, the damage mechanisms, particularly the axial splitting, are not confined to the hole edge, but they are rather distributed over the whole surface and away from the discontinuity. The length of the axial split, which is indicative of the extent and severity of damage, is also noticed to be greater at this temperature. This indicates that damage, particularly the axial splitting becomes more extensive at high temperatures. This observation can be attributed to the degradation in the mechanical properties resulting from the matrix thermal softening which becomes significant beyond the glass transition point.

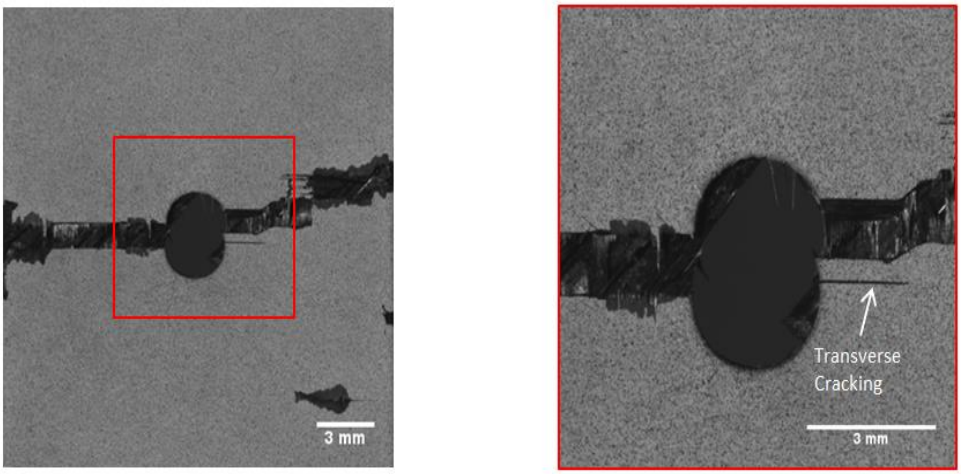

Figure 5.8: Final failure at 25°C

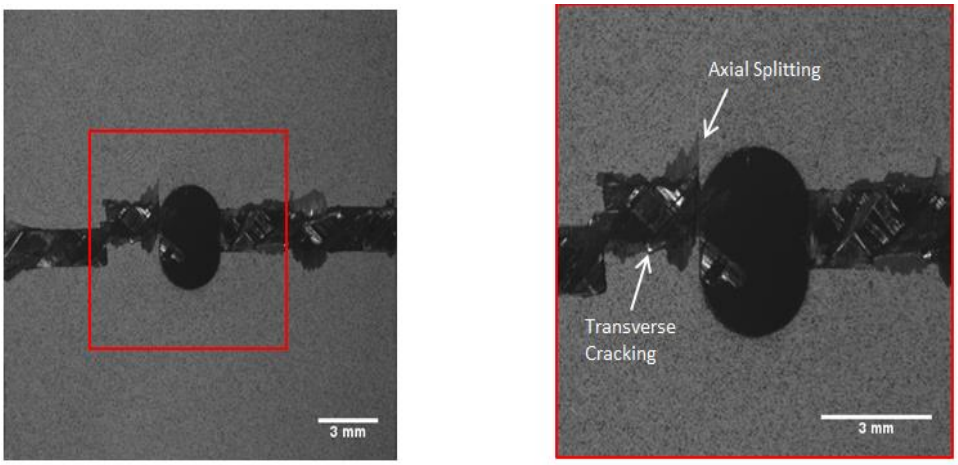

Figure 5.9: Final failure at 50° C

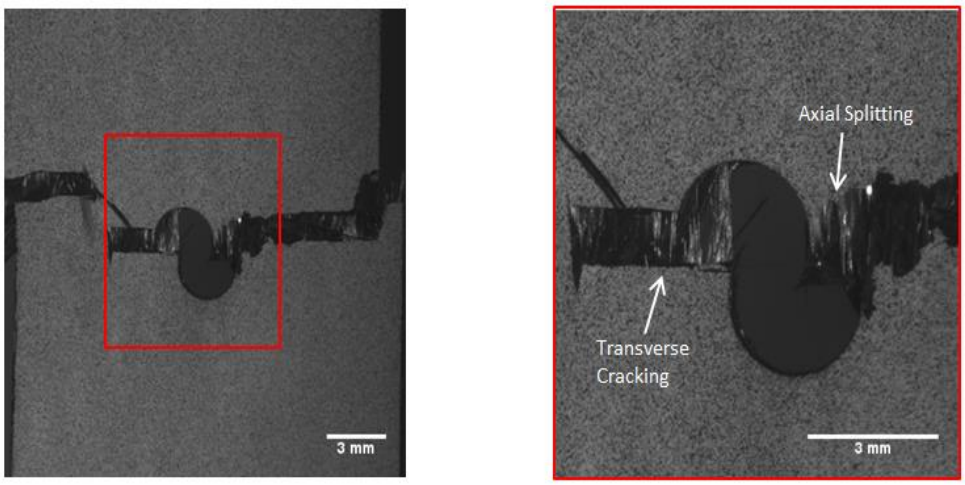

Figure 5.10: Final failure at 75° C

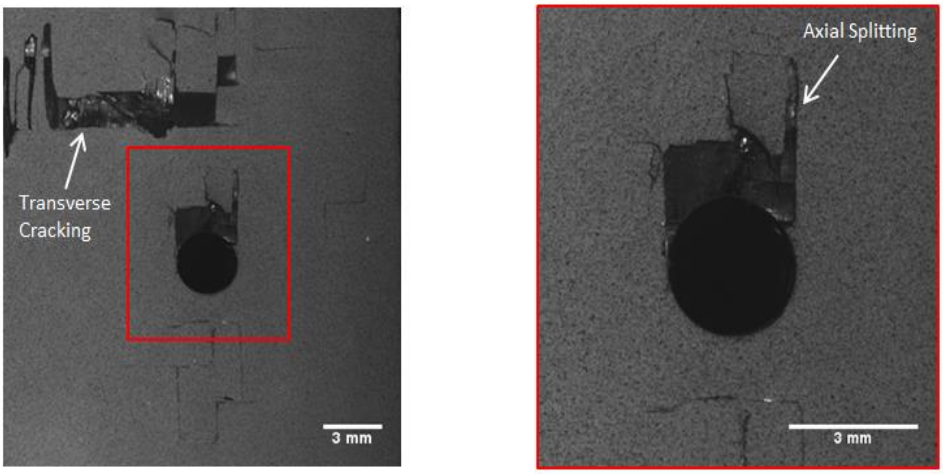

Figure 5.11: Final failure at 100° C

5.4. Effect of Initiation and Progression of Transverse Cracks on the Strain Evolution

To understand the consequence of damage progression on the local and the global response, stress-strain curves of both the local and the nominal regions in the sample tested at RT were plotted in Figure 5.12. To record the vertical local strain (*i.e.*, local strain along the loading direction in the direct vicinity of the drilled holes), virtual DIC extensometer were utilized and placed at the damage initiation site. The stress-strain behavior of the nominal response shows that the material exhibits linear elastic behavior up to failure. However, the stress-strain curve of the local region reveals that the material response is initially elastic up to a stress level of 300 MPa. At this stress level, a transverse crack was detected on the surface of the sample. Beyond this point, the material exhibited an in-elastic behavior and a clear deviation from the linear response. Figure 5.13 shows the damage progression at different stress levels; A, B, and C as highlighted on the local stress-strain curve shown in Figure 5.12. It is noteworthy to mention that the crack initiation was not detected from the global response of the material which highlights the importance of investigating the local response for damage identification.

To monitor the consequence of crack progression on the local response in the neighboring regions of damage initiation site, axial strain in the regions marked with the red and blue boxes was measured and plotted against the nominal stress, as depicted in Figure 5.14. The strain in both regions was observed to increase linearly

with stress till it reaches a strain value of 1.5% and stress level of 270 MPa. Beyond this stress level, a sudden drop in strains was noticed as a consequence of the crack initiation. This indicates that the transverse crack initiation leads to a stress and strain relaxation in the adjacent regions. As explianed previously, such accurate detection and quantification of damage initiation is not available through global and average meaures of deformation and requires, as shown in this work, local analysis of strain accmulation and distribution.

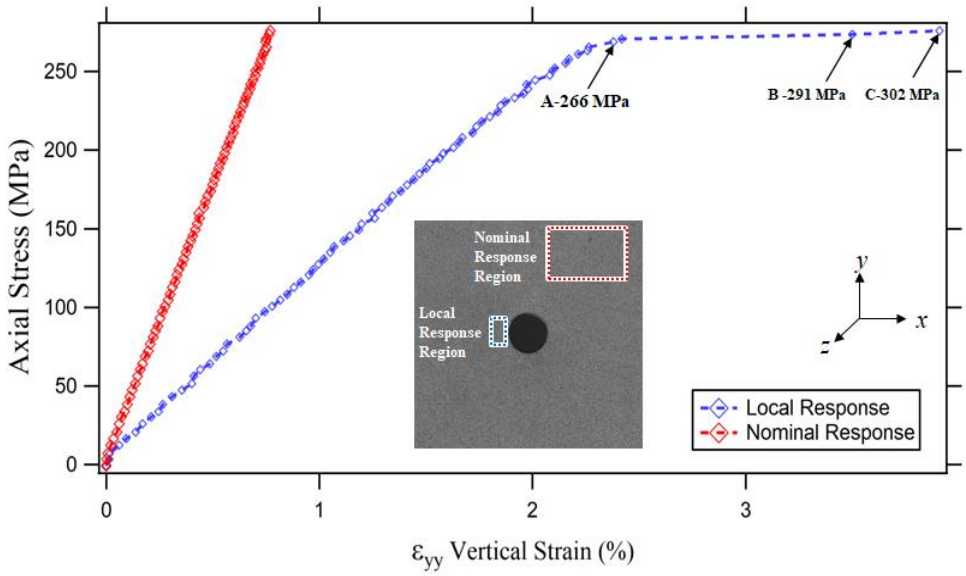

Figure 5.12: Investigating the local response at the crack initiation site

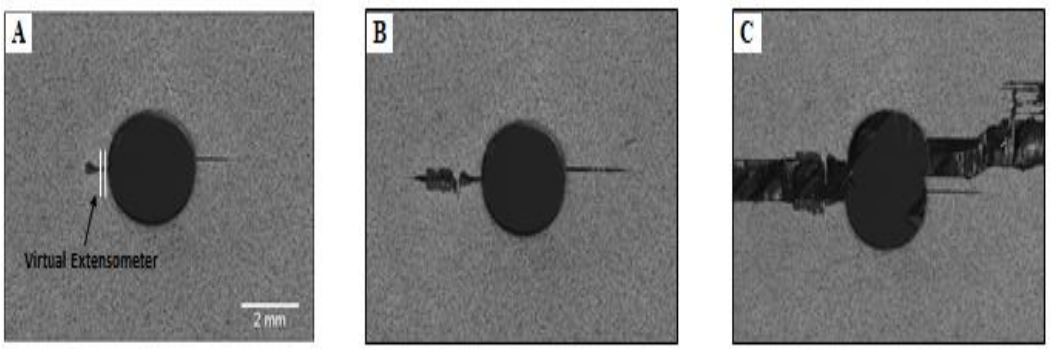

Figure 5.13: Sample images showing the progression of transverse cracks

The local response was also investigated at 50°C, 75°C, and 100° C. The *local* stress-strain curves of the local region at the 4 temperature levels are shown in Figure 5.15. It can be noticed that the stress-strain curves obtained at high temperatures show in-elastic response similar to that obtained at room temperature.

Moreover, the stresss level attained at the onset of the in-elastic response is similar at 25°C and 50°C, while it is noticed to decrease significantly upon increasing the temperature to 75°C and 100°C. It is noteworthy to mention that crack initiation was not clearly evident on the surface of the samples at high temperatures, which shows the effectiveness of DIC measurements in detecting internal cracks (i.e. not evident on the surface) based on the evolution of the strain measurements.

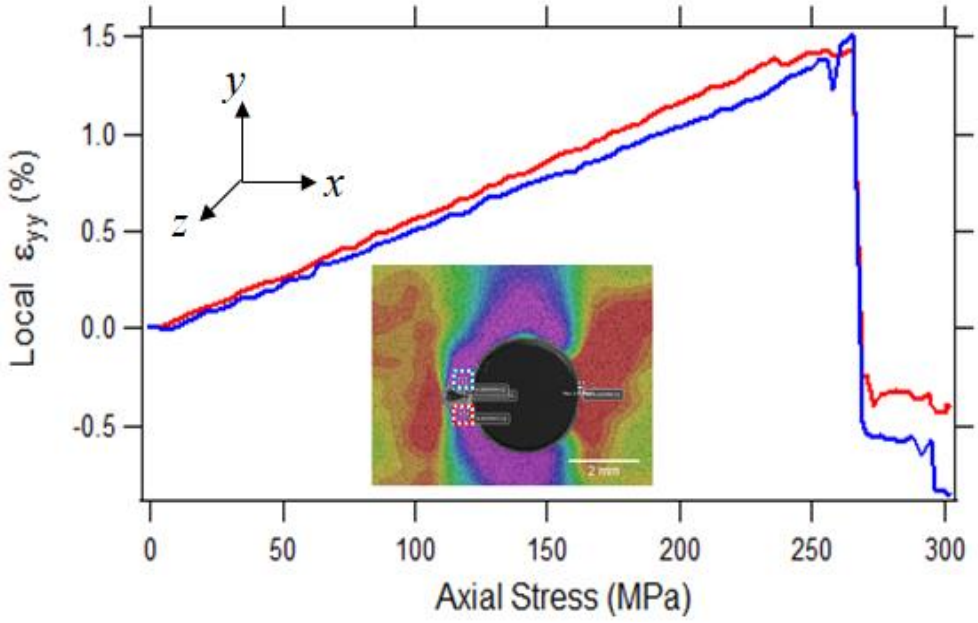

Figure 5.14: Investigating the local response in the neighboring region of the damage

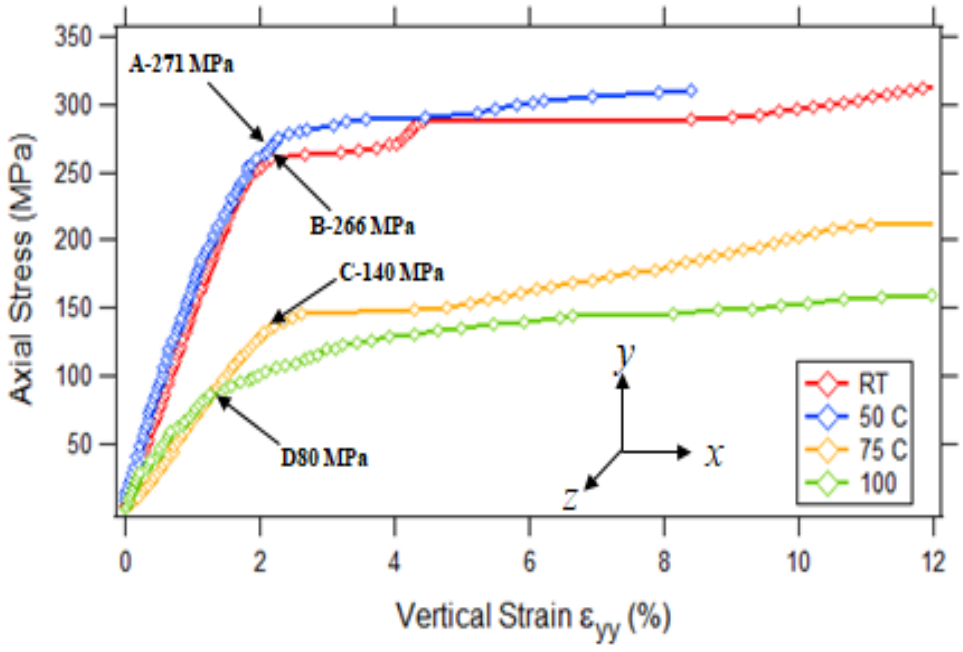

Figure 5.15: Investigating the local response at different temperature levels

5.5 Effect of Axial Splitting Initiation and Progression on the Local Field

Axial splitting damage mode is clearly observed on the surface of the composite sample tested at 75° C. To assess the consequence of damage initation and progression on the local strain field, a small region marked with the red box indicated in Figure 5.16 was inspected. The transverse and the shear strain of this local region were computed using Vic-2D and plotted agianst the axial stress obtained from the load cell in Figures 5.17-5.18. The stress-strain curve of the transverse strains shows that transverse strain is initially negative and decreases linearly with the nominal stress, which can be directly linked to Poisson effect. However, at stress level of 88 MPa, the transverse strain reaches a minimum value after which it starts increasing at an accelerated rate and becomes positive at a stress level of 130 MPa. At the same stress level, a relatively small increase in the rate of change of shear strain can be observed. Moreover, this increase becomes more signifcant at a stress level of 135 Mpa. To relate this change in strain evolution to the damage initiation and progression, images of the sample surface at the aformentioned critical stress levels are dispalyed in Figure 5.19. It can be noticed that at a stress level of 88 MPa and 135 MPa, no sign of axial splitting is observed on the surface. However, at stress level of 180 MPa, where the axial and shear strain values are relatively high, the axial split becomes evident on the surface . Consequently , it can be concluded that the sudden change in strain evolution can be directly linked to the initiation and progression of the axial splitting damage.

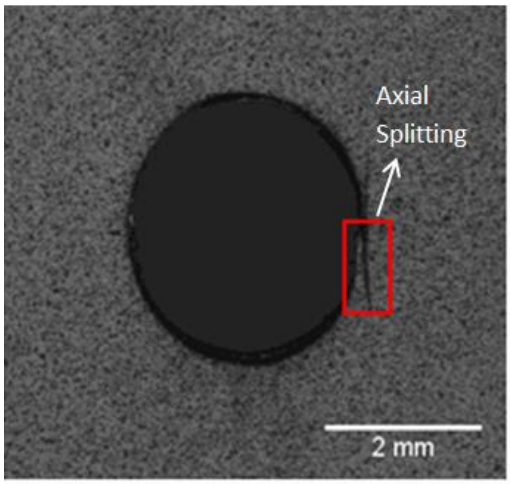

Figure 5.16: Sample image showing axial splitting near the hole edge

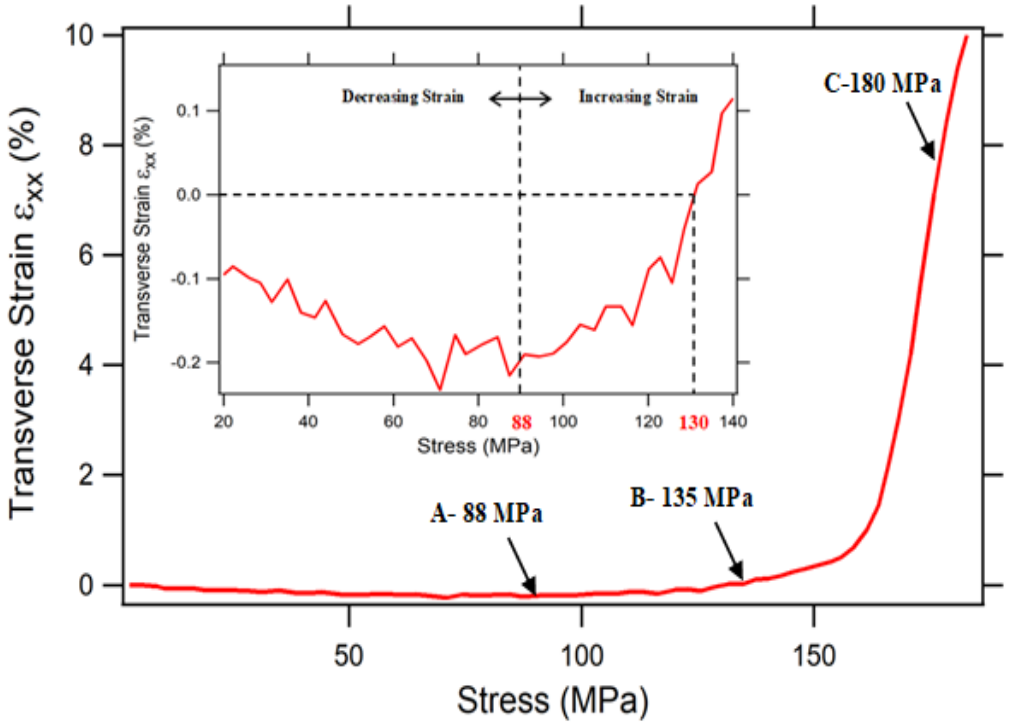

Figure 5.17: Measuring axial strain at the axial splitting initiation site

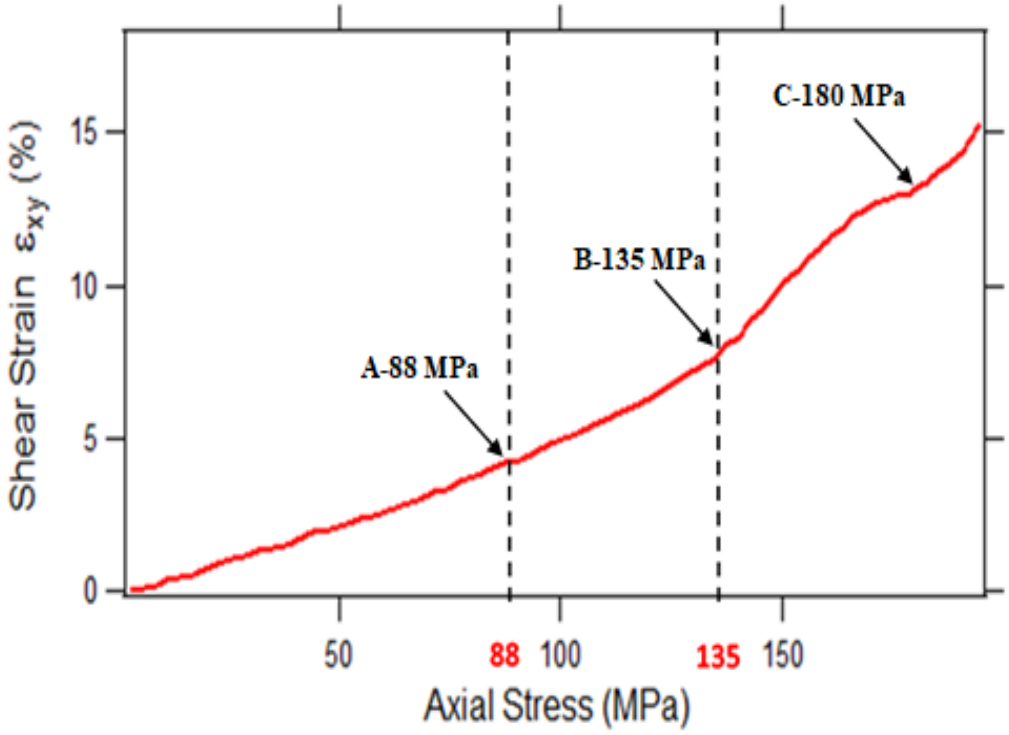

Figure 5.18: Measuring the shear strain at the axial splitting initiation site

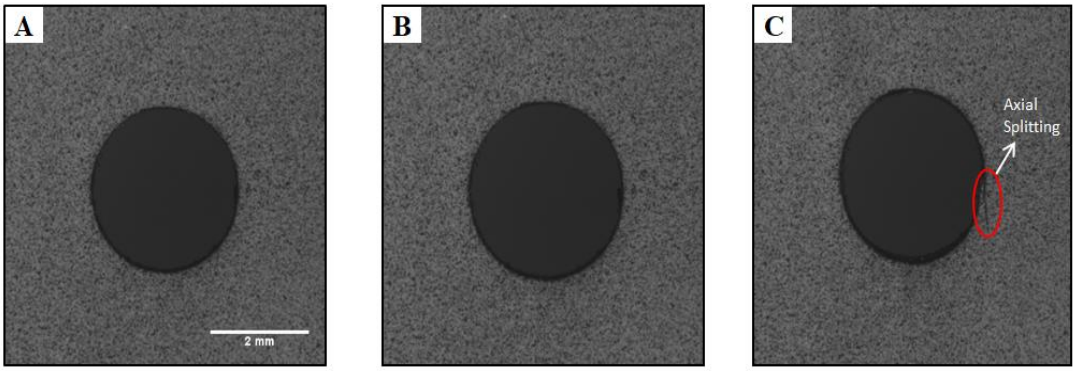

Figure 5.19: Sample images at different stress levels

More importantly, the change in the strain evolution could be utilized to detect damage initiation in cases where axial splitting is not evident on the surface. Thus, `the local transverse strain in the high shear strain region near the hole edge, which is a probable site for damage initiation, was invesigated at 25°C and 50°C.. It should be noted that axial splitting was not evident at the aformentioned temperature. The results are displayed in Figures 5.20-5.22 . It can be noticed that the transverse strain at room temperature remains negative during deformation, and no change in strain evolution was observed, which corresponds well with the observation of the fratured surface which showed the absence of axial splitting at room temperature. However, similar changes in the transverse strain evolution to that observed at 75°C were detected at 50°C. However, the stress level at which the change in strain evolution was observed decreases with the increase in temperature. It can be clearly observed that the sudden change in strain evolution occurs at lower percentage of the ultimate tensile strength at higher temperature. This indicates that high temperatures promotes the early initation and the progression of axial splitting damage mode, allowing for more blunting and stress redistribution to take place.

It has been well reported in the literature that the initiation and progression of axial splitting damage can cause notch blunting (*i.e.* making the notch less sharp by changing the radius of curvature). However, to our knowledge no work has attempted to quantify the blunting effect of axial splitting. Thus, this work aims to address this aspect through measuring the change in hole width during deformation. To achieve that**,** a virtual extensometer was placed along horizontal center line of the hole as depicted in the inset in Figure 5.23. This extenosmeter provides measurments of the

percentage change in the hole diameter during loading. To investigate the effect of axial splitting on the hole gometry, the sample tested at 75°C was first considered, since the axial split was prominent on the surface of the sample at this temperature. The experimental measurement obtained from DIC was plotted against nominal stress as depiceted in Figure 5.23. It was found that initially the hole diameter decreases linearly with strain, which can be directly linked to Possion's effect. However, at the instant when the axial split appeared on the surface, a sudden increase in the hole diameter rate of change was noticed. Subsequently, the hole diameter continued to decrease at a higher rate. This observation indicates that the progression of axial split accelerates the reduction in the hole diameter caused by Possion's effect; thus it blunts the notch. The schematic drawing shown in Figure 5.24 illustrates the consequence of axial splitting on the hole geometry. It can be clearly noticed from Figure 5.24 that initiation and progression of axial splitting in the vicinity of the hole forces the hole boundary inward, resulting in a hole width reduction, and thus an increase in the hole radius of curvature. Consequently, this change in hole curvature will be translated into a reduction in the induced stress concentration near the hole. More importantly, this change in hole diameter can be utilized to detect the progression of axial spitting.

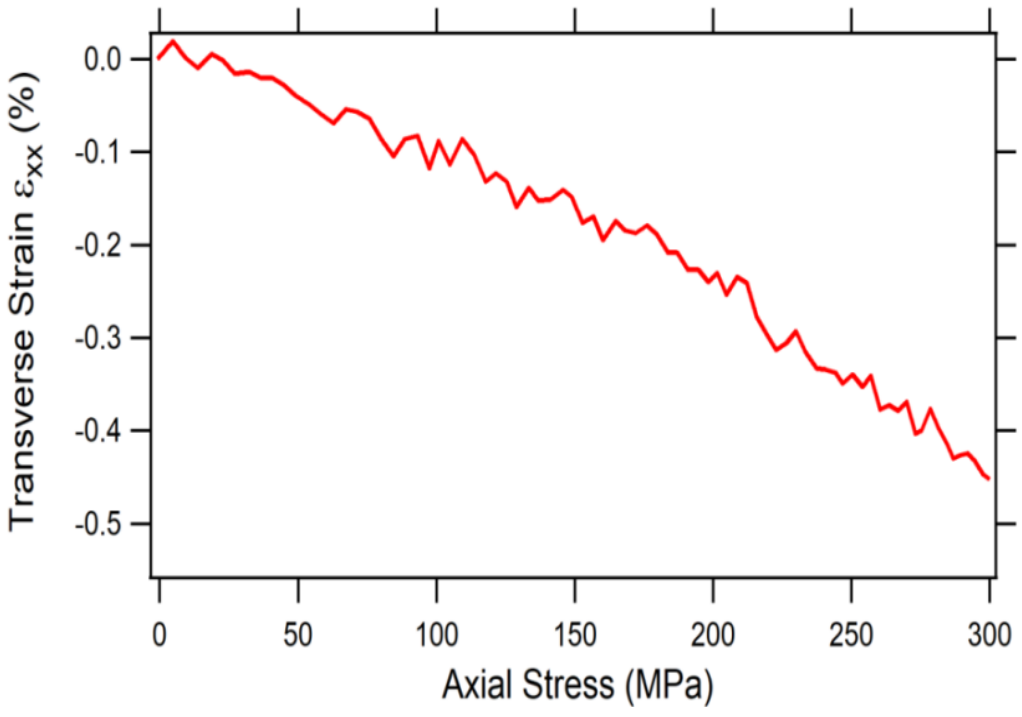

Figure 5.20: Inspecting evolution of transverse strain near the hole edge at 25°C

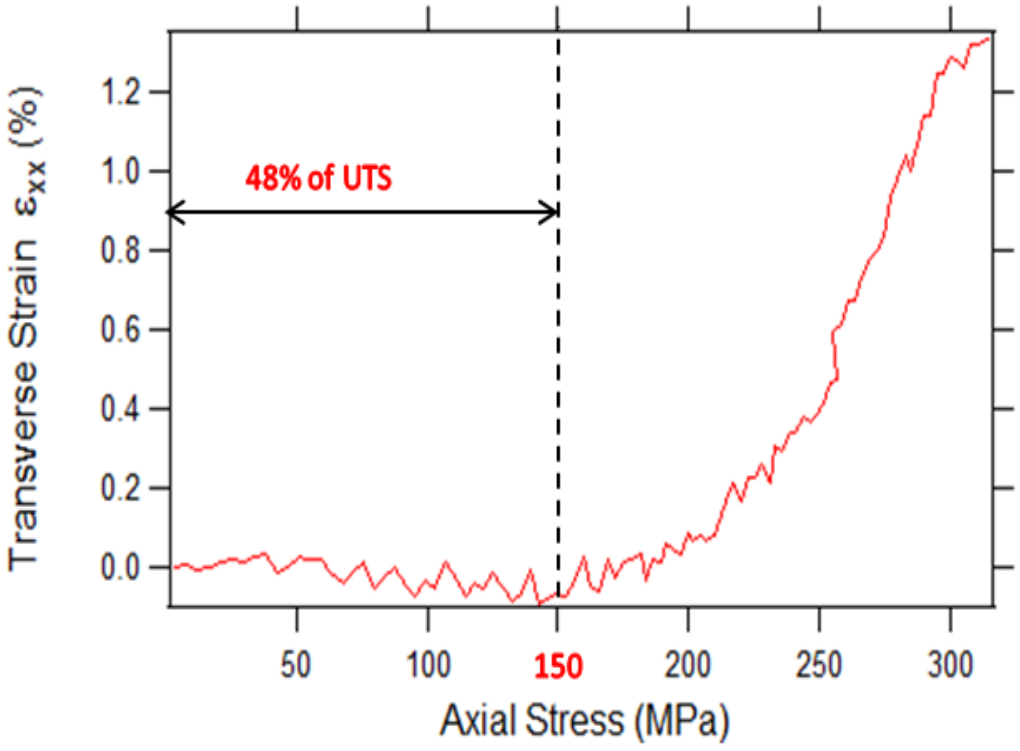

Figure 5.21: Inspecting evolution of transverse strain near the hole edge at 50°C

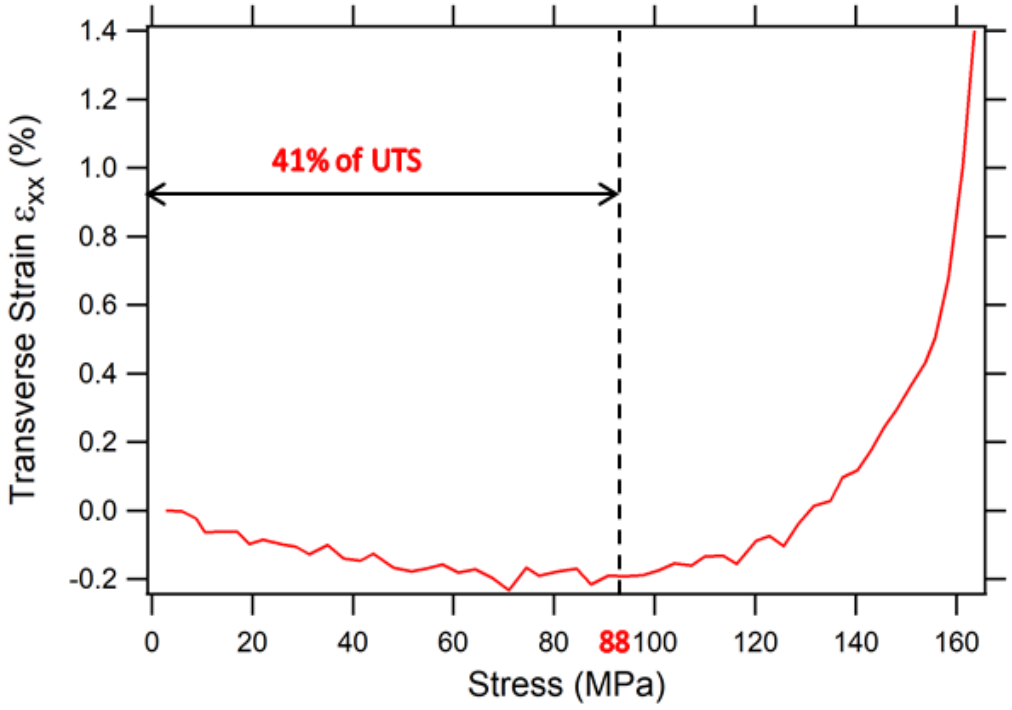

Figure 5.22: Inspecting evolution of transverse strain near the hole edge at 75°C

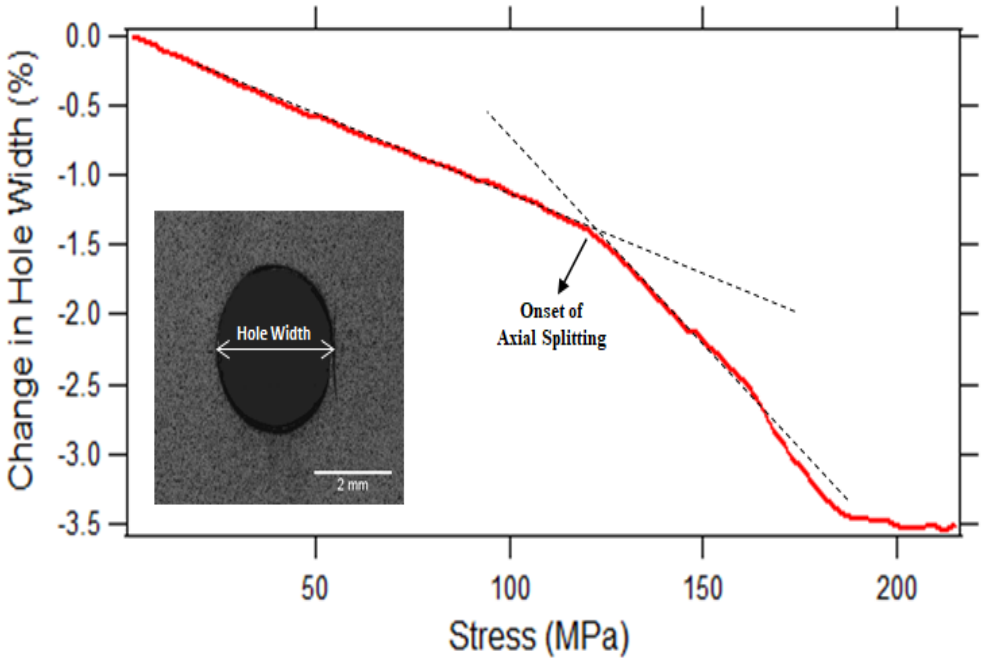

Figure 5.23: Measuring change in hole width as a function of axial stress at 75°C

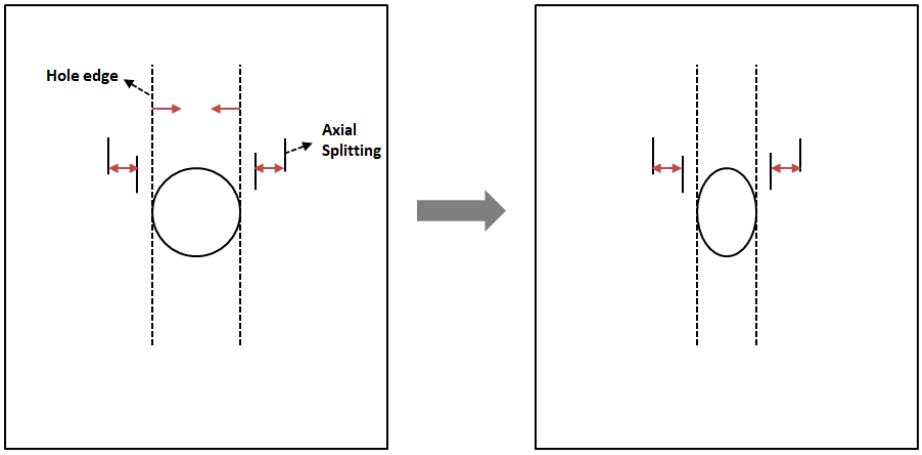

Figure 5.24: Schematic drawing illustrating the blunting effect of axial splitting

To compare the blunting effect at different temperatures, the changes in hole diameter were computed and plotted against the nominal stresses for the samples tested at 25°C, 50°C, and 75°C . The results are displayed in Figure 5.25 . It was found that the rate of change of hole diameter is almost constant at room temperature. This corresponds well with the results obtained earlier which indicates that axial split is not observed at room temperature. However, a sudden increase in the slope of the curve obtained at 50° C is noticed at stress of 240 MPa. It is noteworthy to mention

that the sudden change in the slope is much higher at 75°C than at 50°C indicating that the blunting effect becomes more signifcant at higher temperature. This can be directly linked to the extent of damage which becomes greater at a higher temperature as concluded from previous results.

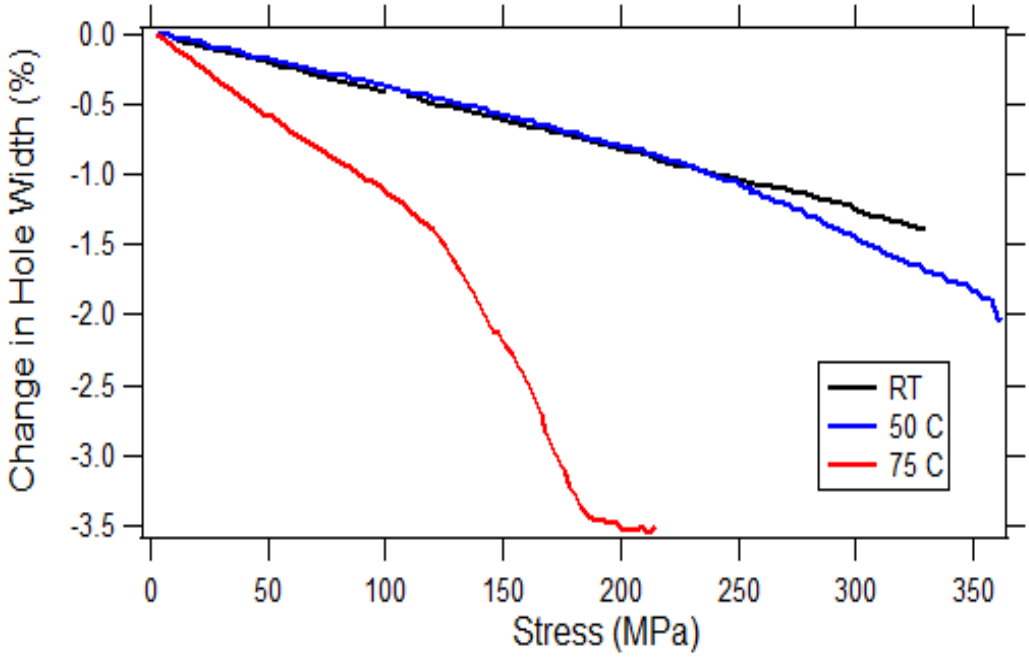

Figure 5.25: Measuring the change in hole width as function of axial stress at different temperature levels

To explore the effect of the axial splitting progression on the neighboring strain field, a small region marked with a red box in Figure 5.26 was inspected. The average axial strian of this region was computed and plotted against the nominal stress, as shown in Figure 5.26. The graph shows a small drop in strain during the evolution of the axial split. This indicates that the progression of the axial splitting causes strain and stress relaxation in the neighboring region of the damage. Consequently, such relaxation can delay the onset of the final failure and hence increase the ultimate tensile strength. This observation ,along with the fact that the axial splitting was evident on the fractured surface at high temperatures, explains well the reduction in the notch sensitivity, observed in section 5.2, with the increase in temperature. Moreover, the unpredicted increase in the ultimate tensile strength at 50° C can be attributed to the initation and progression of axial splitting near the hole edge, which results in a stress relaxation that can delay the onset of the final failure

and negate the consequence of thermal softening, characterized by the drop in the ultimate tensile strength.

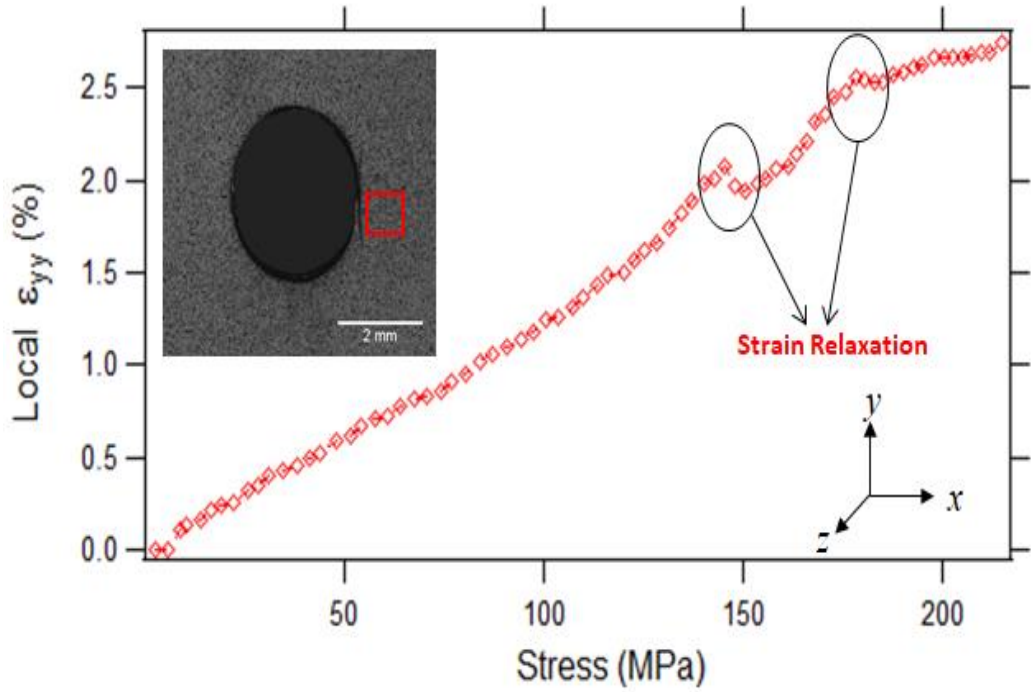

Figure 5.26: Inspecting the local response of neighboring region of the axial splitting

5.6. Residual Strain Evaluation

To assess the local damage induced in the vicinity of the hole, the level of irreversible deformations should be measured. Thus, loading-unloading cycles were applied to samples at the 4 temperature levels. Each sample was first loaded to 90% of the UTS, and then unloaded completely. Subsequently, the shear strain maps, generated at the end of unloading stage, were generated for 25°C, 50°C, and 75°C. The results are depicted in Fig 5.27. It can be noticed that at room temperature, localized shear strain is not observed indicating the absence of irreversible deformations. However, high localized shear strain is evident near the hole edge at higher temperatures, highlighting the presence of localized damage. The residual shear strain observed at high temperatures corresponds to the formation of axial splitting near the hole boundary. To evaluate irreversible strain, the evolution of strain in the small region indicated by the red box was measured during loading-unloading cycle. The results are presented in Figure 5.28. It can be clearly seen that strain attained at the end of the loading stage (i.e. 90% of UTS) increases significantly with

the increase in temperature. This can be attributed to the increase in matrix ductility at higher temperatures. Moreover, the residual strain, measured at the end of the unloading stage, was found to be negligible at room temperature. However, it was noticed to become more significant at higher temperatures. This indicates the increase in temperatures promote the formation of damage in the form of axial splitting in the vicinity of the hole.

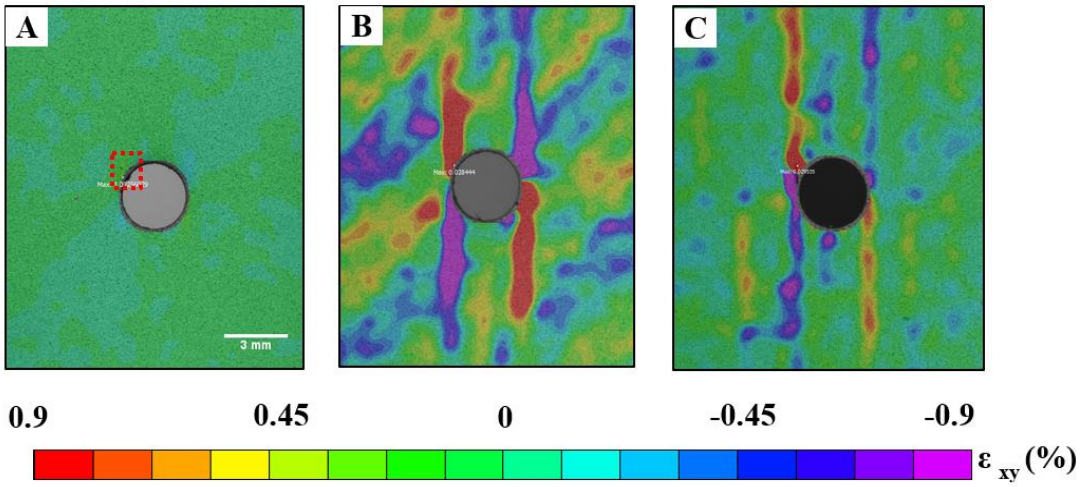

Figure 5.27: Residual shear strain map at A: 25°C, B: 50°C, and C: 75°C

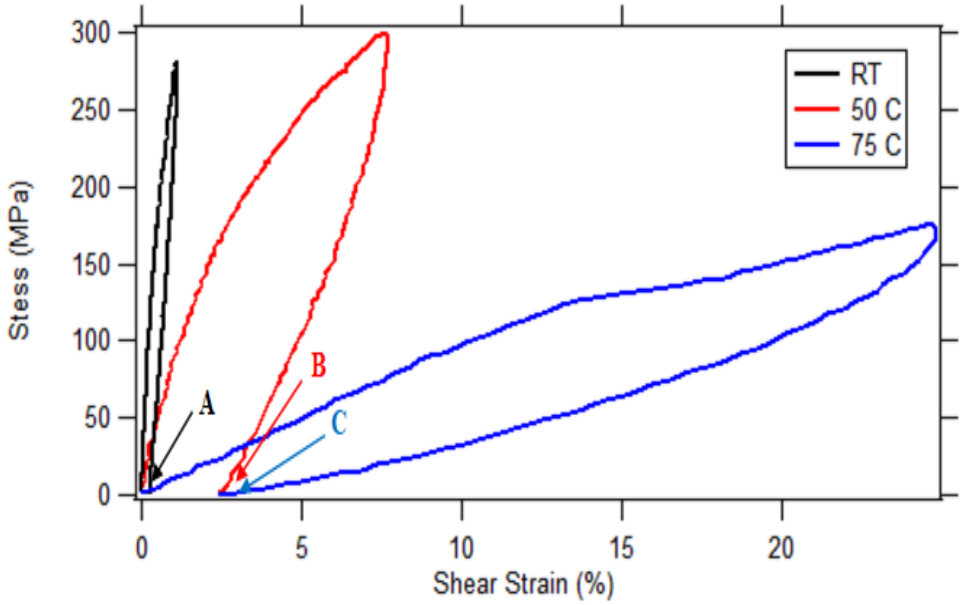

Figure 5.28: Loading-unloading cycle at different temperature levels

5.7. Effect of Damage Accumulation on the Stress Concentration Factor

To further investigate the effect of the inducd localized damage in releiving the stress developed in the vicinity of the hole, notched samples were first loaded to 80% of the ultimate tensile strength, which is high enough to induce localizd damage near the hole, and then unloaded.. A small load was then re-applied to the sample to assess the change in the elastic stress concentration. Subsequently,the experimentally measured strains obtained from DIC were utilized to compute the local axial stresses along the centerline of the circular hole for the first and the second loading. As the laminate tested is orthotropic, the local stresses can be computed using the following planar stress-strain relationships [34]:

$$\begin{bmatrix}\sigma_{xx}\\ \sigma_{yy}\\ \sigma_{xy}\end{bmatrix}=\begin{bmatrix}Q_{xx} & Q_{xy} & 0\\ Q_{xy} & Q_{yy} & 0\\ 0 & 0 & Q_{ss}\end{bmatrix}\begin{bmatrix}\varepsilon_{xx}\\ \varepsilon_{yy}\\ \gamma_{xy}\end{bmatrix} \quad (4)$$

where $Q_{xx}=\frac{E_{xx}}{1-\nu_{xy}\nu_{yx}}$, $Q_{yy}=\frac{E_{yy}}{1-\nu_{xy}\nu_{yx}}$, $Q_{xy}=\frac{\nu_{xy}E_{yy}}{1-\nu_{xy}\nu_{yx}}$ and $Q_{ss}=G_{xy}$

The computed stress is then be divided by the nominal stress to obtain the stress concentration factor.

The results obtained at 25°C and 50°C are presented in Figures 5.29 and 5.30 respectively. It can be clearly seen that good similarity exists between the stress distibutions resulting from the first the second loading at 25°C. It is also worth mentioning that the maximum SCF near the hole edge was similar for both stress distributions. On the other hand, a significant differenrences in the stress distributions resulting from the first and second loading can be noticed for the sample loaded at 50°C. The stress concentration was found to decrease siginifcantly in the second loading. These observation can be attributed to differeneces in the extent and the type of damage developed at each temperatures. It was clear from the examination of the fractured surface that no sign of axial splitting was observed on the surface of the sample. However, inspecting the fractured surface at 50°C indicates the presence of axial splitting in the vicinity of the hole. Moreover, it was clear from the results obtained earlier that the extent of damage, and particularly the axial splitting increases with temperatures, which can consequently lead to higher degree of stress relaxation

near the hole boundary. This justifies the relatively significant reduction in the stress concentration at 50 C during the second cycle.

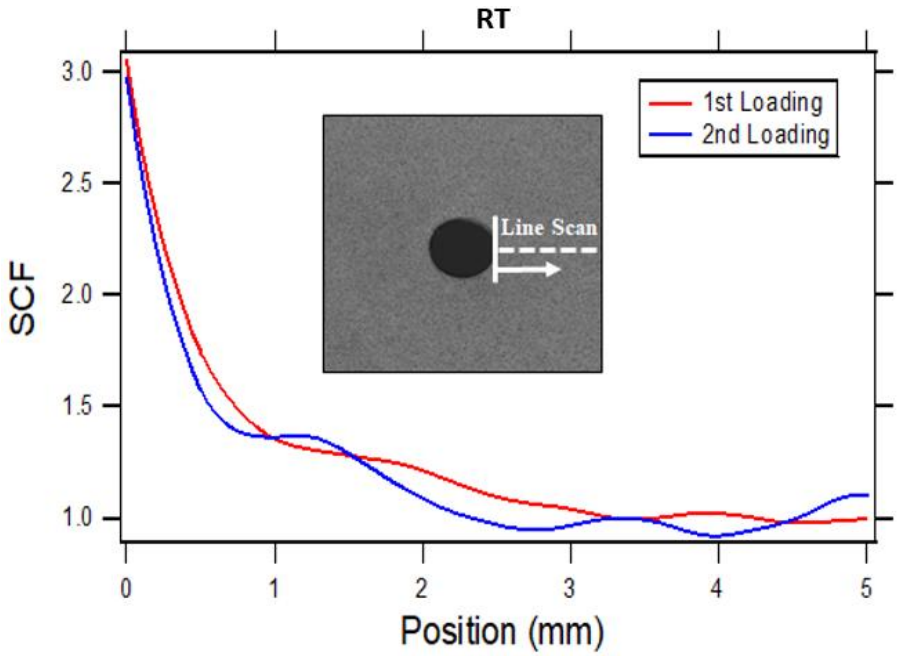

Figure 5.29: Measuring the stress concentration factor along horizontal line passing through the center of the hole at 25°C

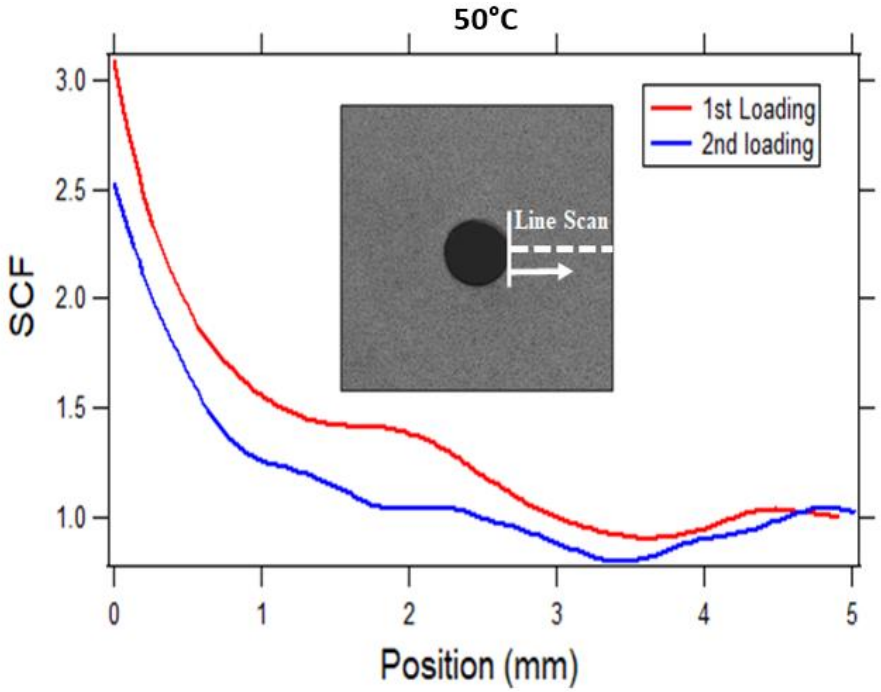

Figure 5.30: Measuring the stress concentration factor along horizontal line passing through the center of the hole at 50°C

Chapter 6. Conclusion and Future Work

The aim of this study was to assess the effect of temperature on the notch sensitivity of woven CFRP composites with circular hole. To satisfy this goal, it was instrumental to monitor the localized response near the hole with the aid of full-field measurement technique. Thus, digital image correlation technique (DIC) was employed to provide different local strain measurements and gain better insight into the damage mechanisms evolved in the vicinity of the hole at different temperature levels. The outcomes of this research can be summarized as follows:

1- Stress-Strain responses of notched and un-notched samples were studied at different temperature levels to ascertain the effect of temperatures on the global behavior of woven CFRP composites. It was shown that the average mechanical properties comprising longitudinal, transverse and shear modulus of elasticity**,** as well as the ultimate tensile strength decrease with the increase in temperatures. However, it was found that the notched tensile strength at 50° C is higher than that at 25°C.

2- Notch sensitivity of CFRP composite was assessed based on the notched to un-notched tensile strength ratio calculated at different temperature levels. The results showed a reduction in this ratio as temperatures increases, indicating that notch sensitivity diminishes at elevated temperatures.

3- Images of the sample final failure were inspected at different temperature levels. Two damage mechanisms were apparent on the surface of the samples, namely axial splitting (*i.e.* longitudinal crack) and transverse cracking. It is worth mentioning that axial splitting was not observed at room temperatures. However, it becomes more extensive with the increase in temperatures, particularly at temperatures well beyond the glass transition point, where the damage was seen to be distributed over the whole surface.

4- Highly localized strain regions were inspected and related to damage initiation and progression. By monitoring the localized strain evolution in the vicinity of the hole, it was shown that localized strain region observed in the axial strain maps can be probable sites for transverse crack initiation. Moreover, the

sudden decrease in the slope of stress-strain curve measured in this region was proved to be an indication of transverse crack initiation.

5- The highly localized shear and transverse strain regions were found to be a probable site for axial splitting initiation. It was shown that a change in the trend of the transverse strain evolution, from decreasing to increasing, was detected at the damage initiation site. Moreover, a sudden increase in the rate of change of shear strain in this region was also observed.

6- To visualize the blunting effect caused by the initiation and progression of axial splitting, the change in hole width was measured as a function of the axial stress at 75°C, where the axial splitting was evident on the sample surface. The hole width measurements indicates that hole width was initially decreasing linearly with the increase in stress due to Poisson's effect. However, a sudden increase in the rate of reduction of the hole width was observed beyond a certain stress level. This sudden change was attributed to the progression of axial splitting. Moreover, the blunting effect was found to become greater at higher temperatures which can be attributed to the increase in the extent of axial splitting driven by the softening effect which allows for higher deformation.

7- To explore the consequence of damage initiation and progression on the local field in the neighboring region of the damage, a small region near the damage initiation was inspected. A reduction in the axial strain was detected during the progression of the axial splitting, highlighting the overstress accommodation that results from damage progression.

8- To assess the extent of the axial splitting damage, a cycle of loading-unloading was applied to samples at 25°C, 50°C, and 75°C. Shear strain maps at the end of unloading stage were generated to visualize the irreversible deformation near the hole edge. It was found that at room temperatures, localized strain region was not evident near the hole edge, while it was clearly observed at 50°C, and 75°C. Moreover, the strain in the localized strain region was measured during the loading-unloading cycle. The stress-strain curves showed negligible residual strain at room temperature compared to 50°C, and 75°C.

The aforementioned results indicate the extent of axial splitting damage becomes greater at high temperatures.

9- To assess the effect of localized damage induced in the vicinity of the hole on the change in the stress concentration caused by the discontinuity, samples at room temperature and 50°C were first loaded to high percentage of the ultimate tensile strength and then unloaded completely. Stress concentration determined from the experimentally measured strain was computed during the first and the second loading. It was shown that unlike the case of room temperature in which minimal changes in stress concentration was observed in the second loading as compared to the first loading, a noticeable reduction in stress concentration of the second loading was observed at 50C. This observation was attributed to the extent and the type of damage that differs between room temperature and 50°C.

As various components in marine and aerospace applications can be subjected to cyclic loading during their service life, it is important to develop a better understanding of the material behavior under fatigue loading, particularly in the presence of discontinuities where different damage mechanisms can evolve and interact in a complex manner. The notched material behavior can be further complicated and probably accelerated at elevated temperatures. Thus, a possible extension of this work is to characterize the synergistic effect of temperatures and fatigue loading on the structural behavior and notch sensitivity of woven composite laminate. This can be performed with the aid of full-field measurement technique to investigate and, most importantly, quantify damage progression near the hole boundaries to develop model capable of predicting the fatigue life of notched composite laminates at different temperature levels.

Moreover, composites parts can be subjected to cyclic temperatures changes which are translated into cyclic thermal stresses. Long time exposure to this thermal cycling can negatively affect the structural integrity and durability of CFRP composites. Thus, a number of studies have been conducted to evaluate the behavior of CFRP composite under thermal cycling. However, few studies have investigated the deleterious effect of thermal cycling in the presence of discontinuity. Accordingly,

a possible subsequent work is to explore the probable synergy between thermal cycling and notches. Moreover, life prediction model that account for both the number of cycles and notch geometry can be developed.

Another possible future work is investigating the creep behavior of notched composite laminate at different temperature levels. Although significant efforts have been devoted to studying the global creep behavior of composite laminate, only few studies have focused on characterizing the local creep behavior near the hole in notched composite laminate. Studying the local behavior can provide deeper insight into the evolution of different damage mechanisms. Moreover, quantifying the damage in the vicinity of the hole can subsequently be utilized to develop damage-based models capable of accurately predicting the creep life of notched composite laminates.

References

[1] P. Lagace, and K. Bonello, "Damage Accumulation in Graphite/Epoxy Laminates Due to Cyclic Gradient Stress Fields," *Journal of Reinforced Plastics and Composites*, vol. 12, no. 10, pp. 1111-1135, October 1993.

[2] R. Zitoune, L.Crouzeix, F. Collombet, T. Tamine, and Y. Grunevald, "Behaviour of composite plates with drilled and moulded hole under tensile load," *Composite Structures*, vol. 93, no. 9, pp. 2384-2391, August 2011.

[3] L. Zhu, N. Li, and P. R. N. Childs, "Light-weighting in aerospace component and system design," *Propulsion and Power Research*, vol. 7, no. 2, pp. 103-119, June 2018.

[4] F. Kahwash, I. Shyha, and A. Maheri, "Machining unidirectional composites using single-point tools: analysis of cutting forces, chip formation and surface integrity," *Procedia engineering*, vol. 132, pp. 569-576, January 2015.

[5] L. Minnetyan, C. Chamis and P. Gotsist, "Damage Progression in Bolted Composites," *Journal of Thermoplastic Composite Materials*, vol. 11, no. 3, pp. 231-248, May 1998.

[6] R. O'Higgins, M. McCarthy and C. McCarthy, "Comparison of open hole tension characteristics of high strength glass and carbon fibre-reinforced composite materials," *Composites Science and Technology*, vol. 68, no. 13, pp. 2770-2778, October 2008.

[7] I. Eriksson, and C. G. Aronsson, "Strength of tensile loaded graphite/epoxy laminates containing cracks, open and filled holes," *Journal of composite materials*, vol. 24, no. 5, pp. 456-482, May 1990.

[8] C. E. Harris, and D. H. Morris, "A fractographic investigation of the influence of stacking sequence on the strength of notched laminated composites," in *STP948 Fractography of modern engineering materials: composites and metals*, J. E. Masters, and J. J. Au, Eds. West Conshohocken, PA: ASTM International, 1987, pp. 131-152.

[9] M. Kortschot and P. Beaumont, "Damage mechanics of composite materials: I—Measurements of damage and strength," *Composites Science and Technology*, vol. 39, no. 4, pp. 289-301, January 1990.

[10] Green, M. Wisnom and S. Hallett, "An experimental investigation into the tensile strength scaling of notched composites," *Composites Part A: Applied Science and Manufacturing*, vol. 38, no. 3, pp. 867-878, March 2007.

[11] C. Harris and D. Morris, "Fracture of thick laminated composites," *Experimental Mechanics*, vol. 26, no. 1, pp. 34-41, March 1986.

[12] T. Coats and C. Harris, "A Progressive Damage Methodology for Residual Strength Predictions of Notched Composite Panels," *Journal of Composite Materials*, vol. 33, no. 23, pp. 2193-2224, December 1999.

[13] J. Wang, P. Callus and M. Bannister, "Experimental and numerical investigation of the tension and compression strength of un-notched and notched quasi-isotropic laminates," *Composite Structures*, vol. 64, no. 3-4, pp. 297-306, June 2004.

[14] J. M. Whitney, and R. J. Nuismer, "Stress fracture criteria for laminated composites containing stress concentrations," *Journal of composite materials*, vol. 8, no. 3, pp. 253-265, July 1974.

[15] M. F. Pinnell, "An examination of the effect of composite constituent properties on the notched-strength performance of composite materials," *Composites Science and Technology*, vol. 56, no. 12, pp. 1405-1413, January 1996.

[16] K. E. Perry, "Delamination and Damage Studies of Composite Materials Using Phase-shifting Interferometry," *Optics and lasers in engineering*, vol. 24, no. 5-6, pp. 467–482, May 1996.

[17] S. R. Hallett and M. R. Wisnom, "Experimental Investigation of Progressive Damage and the Effect of Layup in Notched Tensile Tests," *Journal of Composite Materials*, vol. 40, no. 2, pp. 119–141, January 2006.

[18] M. A. Caminero, M. Lopez-Pedrosa, C. Pinna, and C. Soutis, "Damage monitoring and analysis of composite laminates with an open hole and adhesively bonded repairs using digital image correlation," Composite Part B Engineering, vol. 53, pp. 76–91, October 2013.

[19] F. Pierron, B. Green, M. R. Wisnom, and S. R. Hallett, "Full-field assessment of the damage process of laminated composite open-hole tensile specimens. Part II: Experimental results," *Applied Science and Manufacturing*, vol. 38, no. 11, pp. 2321–2332, November 2007.

[20] C. Au, and O. Büyüköztürk, "Peel and shear fracture characterization of debonding in FRP plated concrete affected by moisture," *Journal of Composites for Construction*, vol. 10, no. 1, pp. 35-47, February 2006.

[21] N. F. Grace, and S. B. Singh, "Durability evaluation of carbon fiber-reinforced polymer strengthened concrete beams: experimental study and design," *ACI Structural Journal*, vol. 102, no. 1, pp. 40-53, January 2005.

[22] W. Liau, and F. Tseng, "The effect of long-term ultraviolet light irradiation on polymer matrix composites," *Polymer composite*, vol. 19, no. 4, pp. 440-445, August 1998.

[23] S. H. Cao, Z. S. Wu, and F. Li, "Effects of temperature on tensile strength of carbon fiber and carbon/epoxy composite sheets," *In Advanced Materials Research*, vol. 476, pp. 778-784, February 2012.

[24] A. Afshar, M. Alkhader, C. S. Korach, and F. P. Chiang, "Effect of long-term exposure to marine environments on the flexural properties of carbon fiber vinylester composites," *Composite Structures*, vol. 126, pp. 72-77, August 2015.

[25] C. Soutis, and D. Turkmen, "Moisture and temperature effects of the compressive failure of CFRP unidirectional laminates," *Journal of Composite Materials*, vol. 31, no. 8, pp. 832-849, October 1997.

[26] J. M. Hale, and A. G. Gibson, "Coupon tests of fibre reinforced plastics at elevated temperatures in offshore processing environments," *Journal of composite materials*, vol. 32, no. 6, pp. 526-543, March 1998.

[27] D. Cree, T. Gamaniouk, M. L. Loong, and M. F. Green, "Tensile and lap-splice shear strength properties of CFRP composites at high temperatures," *Journal of Composites for Construction*, vol. 19, no. 2, pp. 04014043, August 2014.

[28] R. M. Abdalrahman, "Flexural Behavior of CFRP Laminate at Elevated Temperature," *Kurdistan Journal of Applied Research*, vol. 2, no. 3, pp. 330-334, August 2017.

[29] M. J. Shukla, S. Kumar, K. K. Mahato, D. K. Rathore, R. K. Prusty, and B. C. Ray, "A comparative study of the mechanical performance of Glass and Glass/Carbon hybrid polymer composites at different temperature environments," in *IOP Conference Series: Materials Science and Engineering*, vol. 75, no. 1, 2015, pp. 012002.

[30] G. Aklilu, S. Adali, and G. Bright, "Temperature Effect on Mechanical Properties of Carbon, Glass and Hybrid Polymer Composite Specimens," *International Journal of Engineering Research in Africa*, vol. 39, pp. 119-138, November 2018.

[31] G. MAROM, "Environmental effects on fracture mechanical properties of polymer composites," *Composite Materials Series*, vol. 6, pp. 397-424, January 1989.

[32] M. A. Sutton, J. J. Orteu, and H. Schreier, *Image correlation for shape, motion and deformation measurements: basic concepts, theory and applications*. Boston, MA: Springer-Verlag US, 2009.

[33] G. H. Erçin, P. P. Camanho, J. Xavier, G. Catalanotti G, S . Mahdi, P. Linde, "Size effects on the tensile and compressive failure of notched composite laminates," *Composite Structures*, vol. 96, pp. 736-744, February 2013.

[34] A. K. Kaw, *Mechanics of Composite Materials*, 2nd ed. Boca Raton, FL: CRC press, 2005.

Vita

Mostafa Elyoussef was born in 1994 in, Saida, Lebanon. He received his primary and secondary education in Saida, Lebanon. He received his B.E. degree in Mechanical Engineering from the Lebanese American University in 2016.

In September 2016, he joined the Mechanical Engineering master's program in the American University of Sharjah. During his master's study, he co-authored two journal papers. His research interests are in composite materials and shape memory polymers.